

# *Identifying and characterising large ramps in power output of offshore wind farms*

Article

Accepted Version

Creative Commons: Attribution-Noncommercial-No Derivative Works 4.0

Drew, D. R., Barlow, J. F. and Coker, P. J. (2018) Identifying and characterising large ramps in power output of offshore wind farms. *Renewable Energy*, 127. pp. 195-203. ISSN 0960-1481 doi: <https://doi.org/10.1016/j.renene.2018.04.064>  
Available at <https://centaur.reading.ac.uk/76800/>

It is advisable to refer to the publisher's version if you intend to cite from the work. See [Guidance on citing](#).

To link to this article DOI: <http://dx.doi.org/10.1016/j.renene.2018.04.064>

Publisher: Elsevier

All outputs in CentAUR are protected by Intellectual Property Rights law, including copyright law. Copyright and IPR is retained by the creators or other copyright holders. Terms and conditions for use of this material are defined in the [End User Agreement](#).

[www.reading.ac.uk/centaur](http://www.reading.ac.uk/centaur)

**CentAUR**

Central Archive at the University of Reading

Reading's research outputs online

# 1 Identifying and characterising large ramps in power output of 2 offshore wind farms

3 Daniel. R. Drew<sup>1,\*</sup>, Janet. F. Barlow<sup>1</sup> and Phil. J. Coker<sup>2</sup>

4 <sup>1</sup> Department of Meteorology, University of Reading, Reading, UK

5 <sup>2</sup> School of Construction Management and Engineering, University of Reading, Reading, UK

6 \* Author to whom correspondence should be addressed; E-Mail: d.r.drew@reading.ac.uk;  
7 Tel.: +44 (0)118 378 7696

## 9 Abstract

10 Recently there has been a significant change in the distribution of wind farms in Great Britain with the  
11 construction of clusters of large offshore wind farms. These clusters can produce large ramping events  
12 (i.e. changes in power output) on temporal scales which are critical for managing the power system  
13 (30 minute, 60 minute and 4 hours). This study analyses generation data from the Thames Estuary  
14 cluster in conjunction with meteorological observations to determine the magnitude and frequency of  
15 ramping events and the meteorological mechanism.

16 Over a 4 hour time window, the extreme ramping events of the Thames Estuary cluster were caused  
17 by the passage of a cyclone and associated weather fronts. On shorter time scales, the largest ramping  
18 events over 30 minute and 60 minute time windows are not associated with the passage of fronts.  
19 They are caused by three main meteorological mechanisms; (1) very high wind speeds associated with  
20 a cyclone causing turbine cut-out (2) gusts associated with thunderstorms and (3) organised band of  
21 convection following a front. Despite clustering offshore capacity, the addition of offshore wind farms  
22 has increased the mean separation between capacity and therefore reduced the variability in nationally  
23 aggregated generation on high frequency time scales.

24 Keywords: wind; offshore; variability; ramping; extremes

## 25 1.0 Introduction

26 To meet ambitious carbon reduction targets, global renewable energy deployment has expanded  
27 dramatically. In the UK, the capacity of wind power has grown steadily from 2.9 GW in 2008 to 17.9  
28 GW by June 2017 [1]. Due to the increasing penetration of wind power, extreme wind power  
29 generation events are of growing concern. In particular, ramps in generation provide challenges for  
30 the transmission system operator who schedule reserve holding in advance and require long term  
31 strategies for system balancing [2]. Consequently, a number of studies have focused on understanding  
32 and improving the predictability of wind power ramping events [3, 4, 5, 6].

33 For the UK, Cannon et al. [7] used wind speed data derived from the MERRA reanalysis dataset to  
34 quantify the magnitude and frequency of nationally-aggregated wind generation ramping on time  
35 scales of 6 hours and greater based on the 2012 wind farm distribution. However, in recent years there  
36 has been a significant change in the distribution of wind farms in the Great Britain [8]. Since 2012,  
37 the capacity of offshore wind farms has increased from 2.4 GW to 5.0 GW with much of this capacity  
38 spread over a small number of very large wind farms located in clusters. For example, in the Thames  
39 Estuary alone there is approximately 1.7 GW of capacity. Drew et al. [3] showed this has led to large

40 regional ramps in generation on time scales of minutes to hours as local meteorological phenomena  
41 simultaneously impacts production in several large farms. Given the large capacity of the farms, these  
42 ramps can present a challenge in maintaining the balance between supply and demand on a national  
43 scale, particularly if they are not accurately forecasted.

44 The problem posed by local ramping events is expected to be exacerbated in the coming years, given  
45 the trend for clustering capacity in large offshore wind farms looks set to continue. The latest phase of  
46 offshore wind development in the UK, launched in 2009, identified 9 zones within which a number of  
47 individual wind farms could be located with a total capacity of over 30 GW [9, 10]. Consequently,  
48 following the construction of the round 3 wind farms the majority of GB wind capacity would be  
49 located offshore in clusters of very large wind farms [11, 12].

50 To improve the performance of operational wind power forecasts there is an increasing need for a  
51 clear understanding of the meteorological features responsible for the extreme local ramping events  
52 [13]. For example, Trombe et al. [14] showed that high frequency ramping of large Danish offshore  
53 wind farms can be associated with heavy rainfall and therefore considered the scope for using data  
54 from the rainfall radar to adjust the forecast in real-time if necessary. This study investigates whether  
55 such an approach could be applied to ramping events in the Thames Estuary wind farms.

56 In addition to the problems posed by local ramping events, there are concerns that clustering capacity  
57 could lead to an increase in the variability of the nationally aggregated wind generation (i.e. a reversal  
58 of some of the smoothing benefits gained by the spatial dispersion of turbines). A number of studies  
59 have investigated the reduction in wind power variability due to geographical dispersion of turbines  
60 for single European countries. For example, Kubik et al. for Northern Ireland [15], Hurley and  
61 Watson for Ireland [16], Hasche for Germany and Ireland [17] and Giebel [18], Landberg [19],  
62 Buttler [20] and Huber et al. [21] considered the whole of Europe.

63 For the UK, Sinden [22] and Earl et al. [23] used wind speed data measured at Met Office surface  
64 stations to quantify the inter-annual, seasonal and diurnal variability of UK aggregated wind  
65 generation. However, these studies did not consider offshore sites and assumed the distribution of  
66 wind capacity matched the distribution of weather stations which can lead to large errors [24]. To  
67 address this problem, Cannon et al. [7] used wind speed data derived from the MERRA reanalysis  
68 dataset to determine the characteristics of wind power in Great Britain over a 33 year period. The  
69 study provides a detailed climatology of ramping on time scales of 6 hours and greater.

70 Using the approach outlined in Cannon et al. [7], Drew et al. [12] showed that the increased  
71 penetration of offshore wind farms has little impact on the ramping of GB-aggregated wind  
72 generation on time scales of greater than 6 hours. However, due to the resolution of the model,  
73 MERRA reanalysis data cannot be used to determine the high frequency GB-aggregated power  
74 swings (minutes to hours) or quantify the magnitude of wind power ramps at high spatial resolutions  
75 (below 300 km), both of which are important considerations for managing the power system.

76 In the UK, the electricity market is managed in 30 minute windows, known as settlement periods. For  
77 each period, suppliers and generators contract electricity up to 1 hour prior to the delivery time, a cut-  
78 off time known as “gate closure”. It is then the responsibility of the system operator (National Grid) to  
79 take any necessary actions in order to balance the grid within each settlement period. The electricity  
80 network in the UK is largely isolated with relatively few interconnectors to neighbouring countries  
81 and therefore there is a reliance on large conventional power plants to manage the system. However,  
82 these plants generally require a period of notice prior to generation to ramp up, generally assumed to

83 be at least 4 hours. To manage the power system, it is therefore important to understand the possible  
 84 ramps in power that could occur on time scales shorter than the ramp up time of a conventional power  
 85 plant (4 hours), between gate closure and settlement period (1 hour) and from one settlement period to  
 86 the next (30 minutes).

87 The aim of this study is to use a 30-minute averaged time series of wind power generation from a  
 88 number of regions across Great Britain (GB) in 2014 to investigate how the increased penetration of  
 89 clustered offshore wind capacity has affected the characteristics of generation at high spatial and  
 90 temporal resolutions. The first section considers the impact on high frequency variability of wind  
 91 generation on both a national and regional scale, particularly the magnitude of ramping in generation  
 92 on time scales of less than 4 hours. The second section determines the meteorological causes of  
 93 extreme regional ramping events using the Thames Estuary as a case study.

## 94 2.0 Datasets and analysis methods

95 One of the main challenges when investigating the variability of wind generation in the UK at high  
 96 spatiotemporal resolutions is the limited availability of suitable data. Actual metered data from the  
 97 individual wind farms is protected by commercial interests; therefore there is a reliance on nationally  
 98 aggregated data. However, analysis using this data is unable to quantify the regional power swings or  
 99 indicate how the variability has been affected by the change in wind farm distribution. Cradden et al.  
 100 [24] used an hourly 11 year hindcast derived using the Weather Research and Forecasting model  
 101 (WRF) at 3 km resolution to assess the variability of generation from 13 different regions in the UK.

102 This study introduces a new dataset which details the aggregated power output from four offshore  
 103 clusters (Anglia, Cumbria, N.Wales and Thames) and five onshore regions; Argyll, Ayrshire, Central,  
 104 Lothian and SSENW (see Figure 1) at 30 min resolution from 1<sup>st</sup> January 2014 to 31<sup>st</sup> December 2014  
 105 (see Table 1 and Figure 1). The total capacity across the 9 regions is 6.5 GW, which is approximately  
 106 70% of the total installed wind capacity of Great Britain.

107 A number of wind farms have been excluded from the analysis for two reasons (1) they the sole wind  
 108 farm in a region therefore it was not possible to produce anonymous, aggregated generation data or  
 109 (2) the data was not of sufficient quality. Despite the reduced number of wind farms, the dataset  
 110 provides a good representation of the wind resource. For example, the GB-aggregated capacity factor  
 111 for 2014 was calculated to be 31%, which compares well to the figure of 30.2% for the full wind farm  
 112 distribution [25].

	Mean separation (km)	Number of farms	Capacity (GW)
Lothian	17.3	5	0.44
<b>N.Wales</b>	<b>26.9</b>	<b>3</b>	<b>0.18</b>
<b>Cumbria</b>	<b>30.7</b>	<b>5</b>	<b>1.17</b>
<b>Thames</b>	<b>34.5</b>	<b>4</b>	<b>1.54</b>
<b>Anglia</b>	<b>38.1</b>	<b>3</b>	<b>0.33</b>
Central	60.7	11	1.22
Ayrshire	79.3	8	0.52
Argyll	89.1	6	0.30
SSENW	115.2	16	0.80

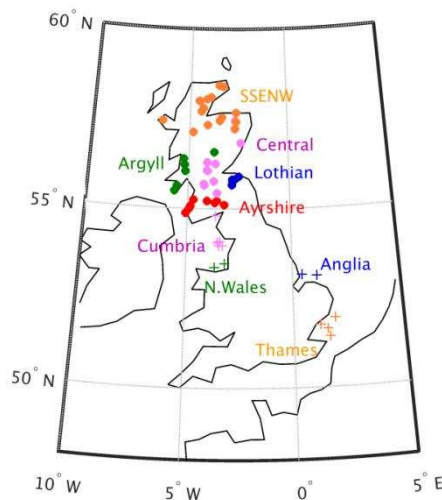
113 **Table 1 Details of the 4 offshore clusters (bold) and the 5 onshore regions. The mean separation is derived using**  
 114 **equation 1 based on the wind farms within each region.**

115 2.1 Spatial separation of capacity

116 The addition of offshore wind farms has changed the distribution of capacity in two distinct ways.  
 117 Firstly, there is an increased concentration of capacity in clusters. For each region the spatial  
 118 dispersion of the capacity has been quantified in terms of the mean separation per unit MW of  
 119 capacity,  $S$ , as calculated in [12] as:

$$s = \sum_{i=1}^N \frac{c_i}{C_T} \left( \sum_{j=1}^N \frac{c_j d_{ij}}{C_T} \right) \quad (1)$$

120 where  $c_j$  is the wind farm capacity,  $d_{ij}$  is the distance between wind farms,  $N$  is the number of wind  
 121 farms in the region and  $C_T$  is the total installed capacity of the region. The offshore regions are  
 122 generally made up of large wind farms clustered together in a relatively small area and consequently  
 123 have a low separation between units of capacity (26.9 km to 38.1 km). In comparison, onshore regions  
 124 generally consist of spatially dispersed small wind farms therefore the separation of the capacity is  
 125 larger (60.7 km to 115.2 km), with the exception of Lothian (17.3 km). Secondly, the addition of the  
 126 offshore regions has changed the geographical location of the generation. Figure 1 shows that all of  
 127 the onshore zones are located relatively close to each other in Scotland; therefore the mean separation  
 128 between the onshore capacity is only 168 km. In contrast, all of the offshore clusters are connected to  
 129 England, and are more geographically dispersed (mean separation of 327.6 km between the offshore  
 130 capacity), therefore by combining the onshore and offshore capacity the mean separation between  
 131 capacity for the GB wind farm distribution increases to 399 km.



132  
 133 **Figure 1 Map of the wind farm distribution used in this study. The onshore and offshore farms are represented by**  
 134 **the circles and crosses respectively.**

135 2.2 Impact of spatial separation on generation characteristics

136 To investigate the impact of spatial separation of capacity on wind power variability in Great Britain,  
 137 the 30-minute averaged time series of aggregated generation for each of the 9 regions have been  
 138 combined to derive a time series of power output for every possible combination of regions. This  
 139 ranges from a combination of two regions (36 possibilities) to the single combination of all nine

140 regions (GB-aggregate) and therefore amounts to a total of 515 possible wind farm distribution  
141 scenarios each with a different number of wind farms and mean separation between capacity. The data  
142 are then used to determine the impact of clustering capacity on the high frequency variability of the  
143 wind generation.

144 A range of different metrics have been used to quantify the variability of wind generation. For the  
145 purposes of this study a ramp,  $R$ , at time,  $t$ , is defined as the difference in the power output over a  
146 period of time,  $\Delta t$ , given by:

$$R(t) = P(t + \Delta t) - P(t) \quad (2)$$

147 where  $P(t)$  is the power output at time,  $t$ . Using the 30-minute averaged dataset, a time series of ramps  
148 for  $\Delta t=30$  minutes, 60 minutes and 4 hours, has been calculated for each wind farm distribution  
149 scenario. The standard deviation,  $\sigma$ , of each time series is then calculated to quantify the distribution  
150 of the ramps for each scenario.

### 151 2.3 Thames Estuary analysis

152 Section 3.3 investigates the most extreme ramping events over three time scales (30 minutes, 60  
153 minutes and 4 hours) of a single offshore cluster in order to determine the meteorological  
154 mechanisms. The analysis focuses on the offshore wind farms in the Thames Estuary, located  
155 approximately 100-200 km east of London, UK. This is the largest of the offshore clusters consisting  
156 of 5 individual farms with a total capacity of 1.7 GW. Drew et al. [3] presents a detailed analysis of a  
157 high frequency ramping event of this cluster which had significant implications on the management of  
158 the power system. This study investigates the full range of extreme ramps to determine the  
159 meteorological cause.

160 To determine extreme ramping events the 30 minute averaged time series of the capacity factor of the  
161 Thames region (as outlined in section 2.2) has been used. The extreme ramping events for each time  
162 window have been defined following a similar method to that outlined in Cutler et al. [6].

- 163 • 4 hour ramps: Find all instances where the 30 minute averaged capacity factor changes by  
164 more than 40% within a 4 hour window. Two individual ramps occurring within a 6 hour  
165 window of each other are considered the same event.
- 166 • 60 minute ramps: After removing the periods of time during which a 4 hour ramp occurs, find  
167 the occasions where the 30 minute averaged capacity factor changes by more than 25% in a  
168 60 minute time window. Two ramps are considered the same event if they occur within 1 hour  
169 of each other.
- 170 • 30 minute ramps: After removing the periods where either a 4 hour or 60 minute ramp occurs,  
171 find the occasions where the 30 minute averaged capacity factor changes by more than 15%  
172 in a 30 minute time window.

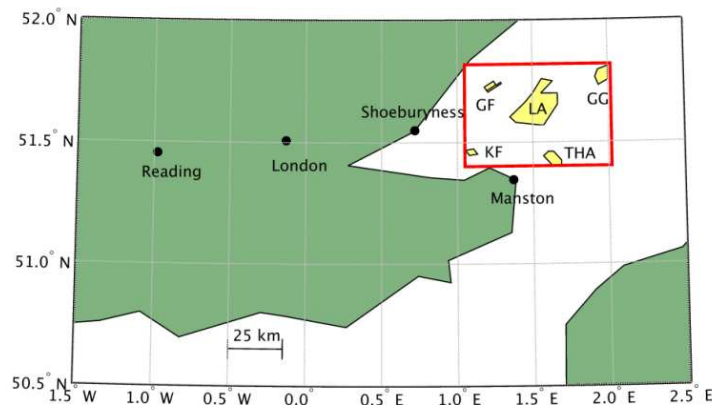
173 To determine the meteorological mechanisms behind extreme ramping events, a number of datasets  
174 have been used (Table 2). Firstly, the meteorological conditions in the Thames Estuary region have  
175 been determined using 1-minute averaged observations of temperature, wind speed and surface  
176 pressure from two nearby Met Office weather stations (shown in Figure 2) and rainfall rate data  
177 derived from radar observations for an area of 4884 m<sup>2</sup> covering all of the wind farms on a 1km<sup>2</sup>  
178 spatial resolution and a 5 minute temporal resolution [26, 27]. On the larger scale, the synoptic scale  
179 conditions have been determined using hourly wind fields and surface pressure from Modern-Era  
180 Retrospective Analysis for Research and Applications (MERRA) data [28].

181 In addition to determining the meteorological conditions associated with ramps, hourly surface wind  
 182 field data from MERRA has been used to estimate the aggregated power generation of the wind farms  
 183 in the region, following the method of Cannon et al. [7]. Firstly, the horizontally gridded surface  
 184 hourly winds were bi-linearly interpolated to the location of each wind farm. The derived winds were  
 185 then vertically interpolated to the hub height of the turbines. Finally, the hub-height wind speeds were  
 186 converted to power output using a transfer function derived from empirical comparisons between the  
 187 derived wind speeds and recorded wind farm output. The power output was summed over all wind  
 188 farms to produce an hourly time series of generation of the Thames Estuary cluster.

189

Dataset	Variables	Temporal resolution	Location
UK Met Office weather station observations	Air temperature (C) at 1.25 m above the ground. Mean wind speed and maximum gust at 10 m above the ground ( $\text{ms}^{-1}$ ). Atmospheric pressure (hPa).	1-minute	Manston (51.346°N, 1.337°E).and Shoeburyness (51.536°N, 0.809°E).
Met Office rainfall radar	Rainfall rate ( $\text{mm hr}^{-1}$ )	5-minute	Thames Estuary region (see Figure 2) on $1 \text{ km}^2$ resolution.
MERRA: Modern-Era Retrospective Analysis for Research and Applications	Mean wind speed ( $\text{ms}^{-1}$ ) at heights of 2 m, 10 m and 50 m. Surface pressure (hPa).	Hourly	$0.5^\circ \times 0.667^\circ$ global grid.

190 **Table 1 Details of the meteorological datasets used in this study.**



191

192 **Figure 2 Map showing the location of the 5 wind farms in the Thames Estuary: Greater Gabbard (GG), London**  
 193 **Array (LA), Gunfleet Sands (GF), Kentish Flats (KF) and Thanet (THA). The red box indicates the region for which**  
 194 **radar rainfall data was obtained. The map also shows the locations of the surface meteorological stations:**  
 195 **Manston and Shoeburyness.**

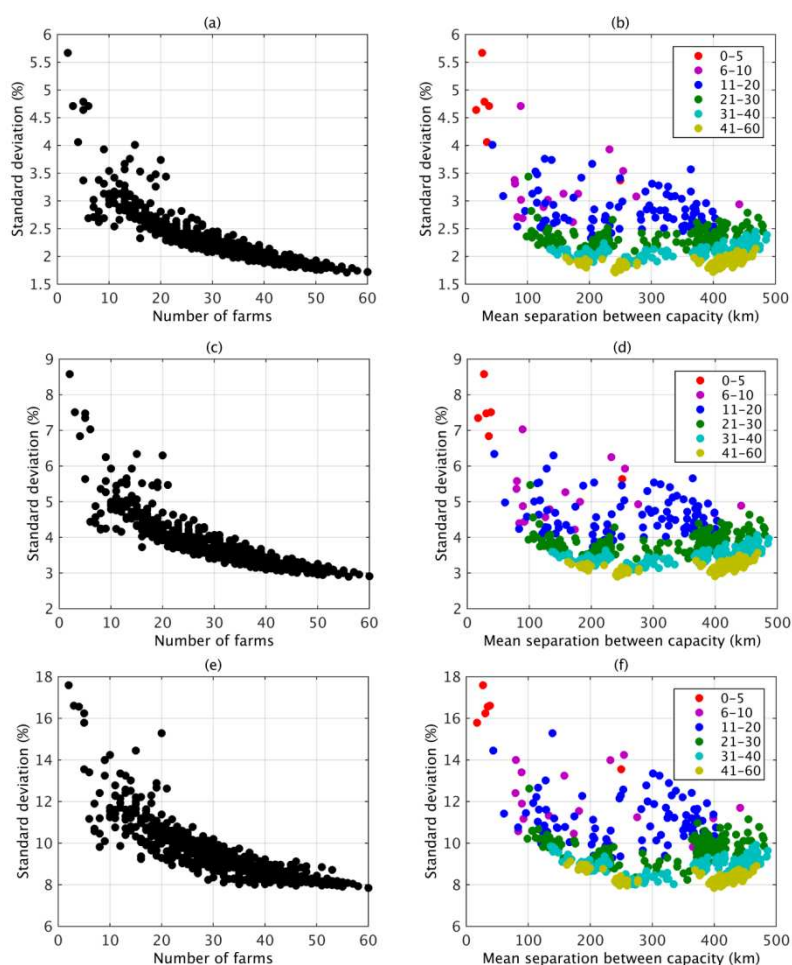
### 196 3.0 Results

197 The dataset outlined in Section 2 has been used to address a series of questions related to wind power  
 198 variability. Section 3.1 investigates the impact of the offshore wind farms on the GB-aggregated wind  
 199 generation characteristics, with a particular emphasis on the impact of changing the separation  
 200 between capacity and the number of wind farms on the magnitude on the high frequency ramps.  
 201 Section 3.2 determines the magnitude of regional high frequency power swings for the offshore

202 clusters and compares the results to that of the more spatially-dispersed onshore regions. Finally,  
 203 Section 3.3 quantifies the high frequency ramping of wind farms in the Thames Estuary, the largest  
 204 offshore cluster and identifies the meteorological mechanism.

### 205 3.1 Impact of clustering capacity on generation variability

206 This section determines how the magnitude of the ramps in regional wind power varies with two  
 207 metrics used to define the level of clustering (1) the number of wind farms aggregated and (2) the  
 208 mean separation between capacity. For all 515 possible wind farm distributions, the time series of  
 209 power ramps over three time periods (30 minutes, 60 minutes and 4 hours) have been determine. The  
 210 standard deviation of the resulting time series was calculated and is used as a measure of the  
 211 magnitude of the ramps.



212  
 213 **Figure 3 Standard deviation of the power ramps of each of the 515 different wind farm distributions as a function of**  
 214 **the number of farms in the distribution and the mean separation between the capacity for three time windows (a)-(b)**  
 215 **30 minutes, (c)-(d) 60 minutes and (e)-(f) 4 hours.**

216 For all three time scales, the magnitude of the ramps decreases as the number of wind farms in the  
 217 distribution increases (see Figures 3(a)-(f)). A large reduction in the standard deviation is shown  
 218 between 5 and 30 wind farms before levelling off as the number of farms increases further. For  
 219 example, for the 30 minute ramps the standard deviation decreases from approximately 4.8% to 2.1%  
 220 as the number of wind farms increases from 5 to 25, but decreases to only 1.9% as the number of  
 221 wind farms increases further to 50. However, for all time scales the lowest standard deviation is  
 222 shown for the largest number of wind farms (i.e. the full GB wind farm distribution).



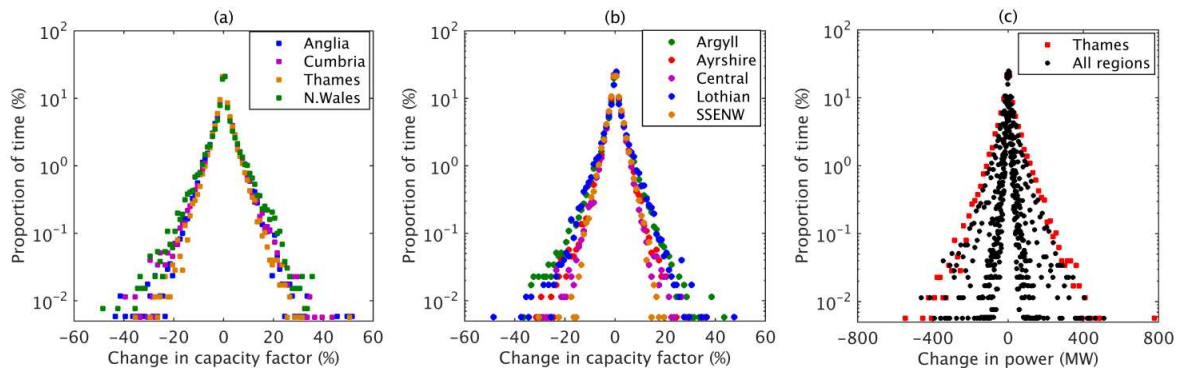
223 This analysis indicates that the number of wind farms aggregated is a useful parameter for estimating  
224 the distribution of power swings on time scales of 30 minutes to 4 hours. In comparison, the  
225 separation between capacity is not a good indicator of the size of the ramps. For all time scales,  
226 increasing the separation (but keeping the number of wind farms the same) has little impact on the  
227 size of the ramps (see Figures 3(b), 3(d) and 3(f). For example, for a wind farm distribution which  
228 contains 41-60 farms, if the separation between the units of capacity is 200 km the standard deviation  
229 of the 30 minute ramps is between 1.8% and 2.0%. If the separation were to increase to 400 km the  
230 standard deviation is very similar (1.7% - 2.0%). These results suggest that on the time scales  
231 considered, the power ramps of the regions are not well correlated, therefore the magnitude of the  
232 aggregated ramps decrease as more and more regions (number of farms) are added, irrespective of any  
233 potential change in the separation between capacity.

### 234 3.2 Regional power ramps

235 The analysis in section 3.2 has shown that the magnitude of the power ramps of a wind farm  
236 distribution is highly dependent on the number of wind farms. The recent trend of concentrating a  
237 small number of very large wind farms therefore results in an increase in the magnitude of the local  
238 power ramps. Figures 4 to 6 show the distribution of the power ramps for each region in Great Britain  
239 in 2014. For all time intervals, the distribution is approximately symmetric with median values close  
240 to zero for both the onshore and offshore regions, indicating that positive and negative ramps have a  
241 similar distribution.

242 In general, when considered in terms of a change in capacity factor, the magnitude of the ramps is  
243 larger for the offshore clusters for all time scales. Consequently, if the system operator were to hold  
244 reserve to protect against a 90th percentile swing, for the onshore regions it would equate to on  
245 average 3.8%, 6.0% and 14.5% of capacity for 30 minutes, 60 minutes and 4 hours respectively. In  
246 comparison a similar holding for the offshore regions would equate to an average of 4.8%, 7.9% and  
247 18.9% of capacity. This is due to the offshore clusters containing a lower number of farms than the  
248 onshore zones. As the 4 offshore regions have a similar number of farms, the magnitude of ramps is  
249 very similar for all offshore regions- with slight differences in the extreme values. For the onshore  
250 regions, there is generally a larger spread in the distributions reflecting the variability in the number of  
251 farms across the regions. For example, for Lothian there are a similar number of wind farms to the  
252 offshore regions and the standard deviation of the ramps is 4.7%, 7.6% and 17.9% for 30 minutes, 60  
253 minutes and 4 hours respectively.

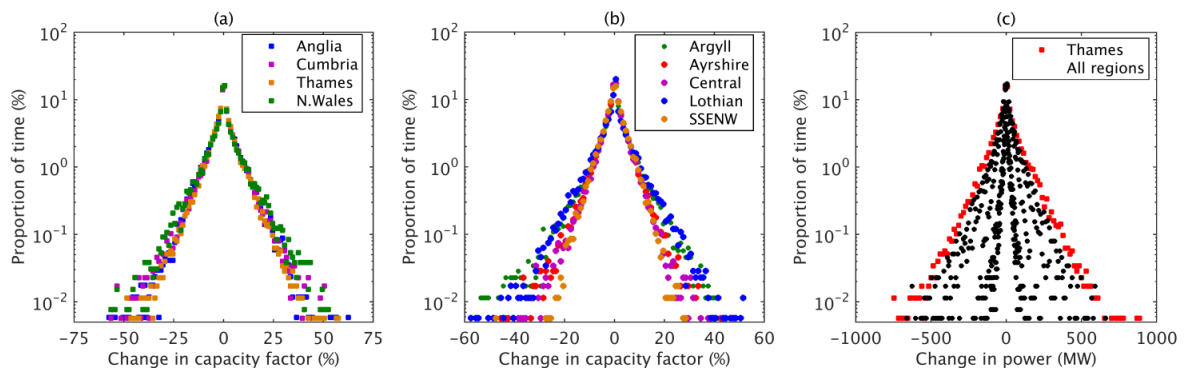
254 When considered in terms of change in power (MW), due to large capacity in Thames Estuary, the  
255 ramps of the cluster are larger than all other regions for all time scales (as shown in Figures 4-6 (c)).  
256 For example, for the 30 minutes, 60 minutes and 4 hour time window, the maximum ramp in the  
257 Thames Estuary is 777 MW, 886 MW and 1363 MW. Power ramps of this magnitude could  
258 potentially pose a challenge to those responsible for maintaining a balance between supply and  
259 demand on the power system. Accurate meteorological forecasting is critical to decisions made on  
260 holding reserve, but can be difficult on such short timescales. Here follows a detailed investigation  
261 into the meteorological conditions causing ramps in the Thames Estuary, to inform development of  
262 accurate forecasts.



263

264  
265

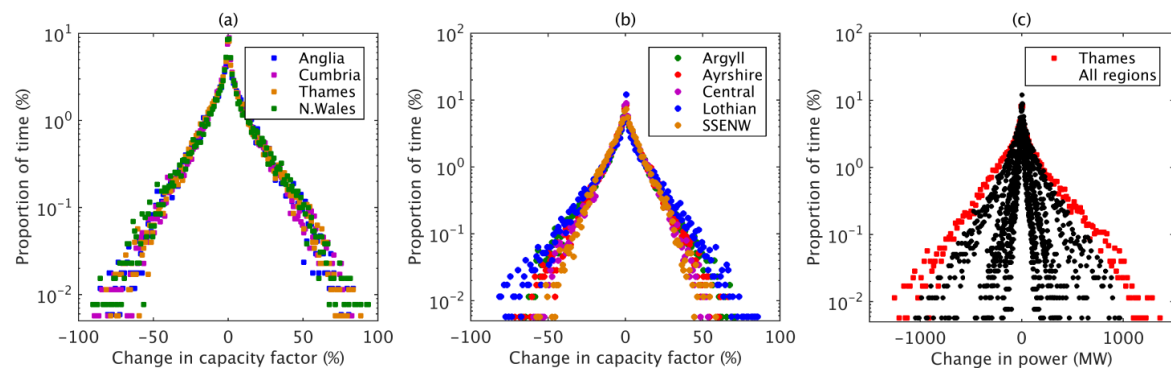
**Figure 4** Distribution of the change in capacity factor within a 30 minute time window in 2014 for (a) offshore clusters (b) onshore regions. (c) The ramps expressed in terms of power (MW).



266

267  
268

**Figure 5** Distribution of the change in capacity factor within a 60 minute time window in 2014 for (a) offshore clusters (b) onshore regions. (c) The ramps expressed in terms of power (MW).



269

270  
271

**Figure 6** Distribution of the change in capacity factor within a 4 hour time window in 2014 for (a) offshore clusters (b) onshore regions. (c) The ramps expressed in terms of power (MW).

### 272 3.3 Thames Estuary ramping

273 In Section 3.2 it was shown that the clusters of offshore wind farms can lead to large high frequency  
 274 regional power ramps. This section analyses the generation data from the Thames Estuary cluster (the  
 275 largest of the offshore clusters in terms of capacity) in more detail, to identify the extreme ramping  
 276 events and determine the meteorological drivers. As with the previous sections, the analysis has been  
 277 completed on three time scales (30 minutes, 60 minutes and 4 hours).

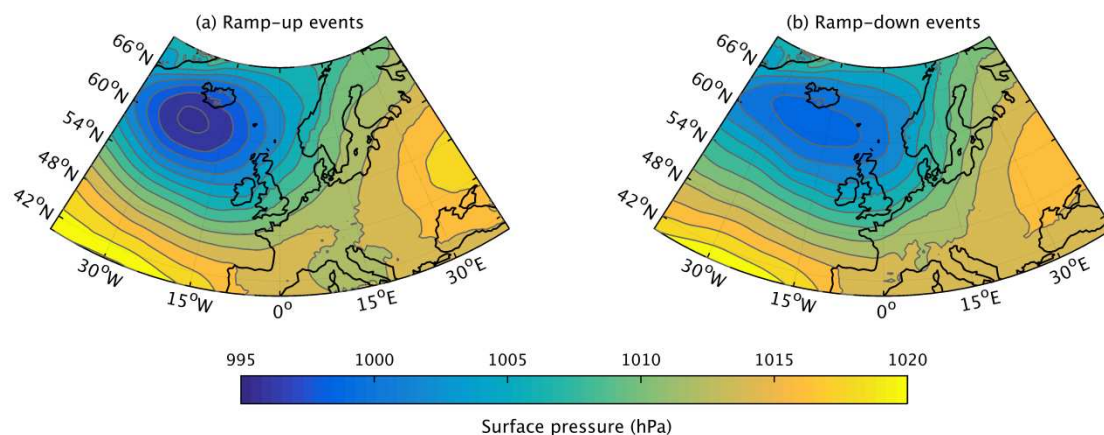
#### 278 3.3.1 Extreme ramps over a 4-hour time window

279 Following the method outlined in section 2.3 (the hourly capacity factor changes by more than 40%  
 280 over a 4 hour time window), 74 ramp-up events and 69 ramp-down events were identified. Events  
 281 occurred throughout the year, however a larger proportion occurred in winter (39% in DJF) than any

282 of the other seasons (22% in MAM, 24% in JJA and 15% in SON). The most extreme ramp-up event  
283 was 86.2% which equates to a change in power of 1.3 GW and the most extreme ramp-down was  
284 76.7% which equates to a change in power of 1.2 GW.

285 For each event, the synoptic meteorological conditions have been investigated using the surface  
286 pressure data from MERRA (see figure 7). All of the extreme ramping events on this time scale can  
287 be linked to the passage of an extra-tropical cyclone (low pressure system) and the associated weather  
288 fronts. For all of the 74 ramp-up events, there is a clear pattern in the surface pressure field. A low  
289 pressure system is centred over Iceland and the frontal features stretch south-east across the UK.  
290 There is a similar pattern for the ramp-down events however the centre of the low pressure has moved  
291 eastwards and the gradient in surface pressure over the UK has weakened. Additionally, the frontal  
292 features are now located east of the cluster.

293 By applying the method developed in Cannon et al. [7], the hourly generation of the Thames Estuary  
294 cluster in 2014 has been estimated based on the surface wind field given by MERRA. The derived  
295 data have been analysed to determine whether extreme ramping events are captured. MERRA is  
296 defined to have captured a ramp if it is at least 75% of the size of the measured ramp within a  $\pm 3$  hour  
297 time window of when it occurred. Based on this criterion, the MERRA derived data captures all 74  
298 ramp-up events and 69 ramp-down events which occurred in the Thames Estuary offshore cluster  
299 during 2014. This confirms that the extreme ramping on this time scale is the result of synoptic scale  
300 meteorological features which are well reproduced by the reanalysis product.

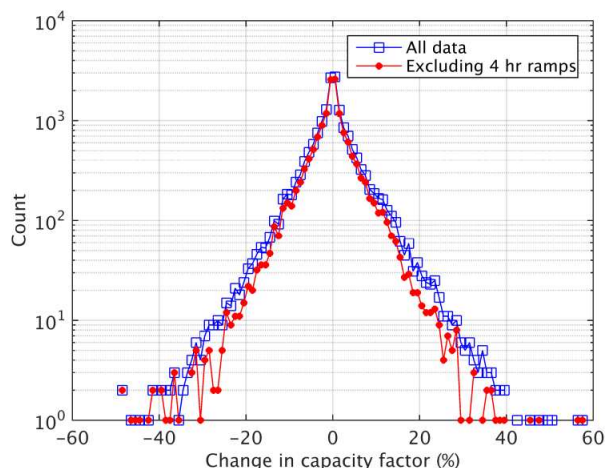


301

302 **Figure 7 Mean sea level pressure averaged across all (a) 74 ramp-up events and (b) 69 ramp-down events.**

### 303 3.3.2 Extreme ramps over a 1-hour time window

304 For the full year of measured data, power ramps over a one hour time window have been calculated  
305 and the frequency distribution of the ramps is shown in Figure 8 (this is the same data as the Thames  
306 curve in Figure 5(a)). The data have then been filtered to remove the periods which contain a 4 hour  
307 ramp (identified in section 3.3.1) and the distribution of the filtered ramps is also shown in Figure 8.  
308 A comparison of the probability density functions shows the most extreme 60 minute ramping events  
309 are the same in both distributions. For the both the filtered and unfiltered datasets the largest ramp-  
310 down is -48.8% and the largest ramp-up event is 57.9%. This indicates that the most extreme 1 hour  
311 ramps are not part of a larger scale ramp and are therefore not caused by the passage of low pressure  
312 system but by smaller scale meteorological features.



313

314 **Figure 8 The 60 minute ramps for the Thames Estuary cluster during 2014 using the whole dataset (blue) and then**  
 315 **excluding the periods during which a 4 hour ramp occurs.**

316 Using the criteria outlined in section 2.3, 24 x 1 hour extreme ramping events have been identified.  
 317 Further analysis shows, on 10 occasions an extreme ramp-up and ramp-down occurred within 3 hours  
 318 of each other (as shown in Table 3). These ramps were combined to produce 14 independent events.  
 319 For each event, the meteorological conditions have been investigated using surface pressure fields  
 320 from MERRA, observations of surface temperature and wind speed from Met Office weather stations  
 321 close to the cluster (Manston and Shoeburyness) and rainfall radar data. Based on the meteorological  
 322 data, 3 main drivers of the extreme ramping on this time scale have been identified; (1) turbine cut-out  
 323 due to high wind speed conditions (2) outflow or gust fronts from thunderstorms and (3) organised  
 324 band of convection following a frontal system.

### 325 3.3.3 High wind speed cut-out

326 There were 5 ramping events associated with the high wind speed shutdown of turbines. The largest  
 327 of which occurred on 14<sup>th</sup> February 2014, when the output of the farms reduced by 44.3% (i.e. a  
 328 reduction in power output of 680 MW in 1 hour). All 5 of the cut-out ramping events occurred in  
 329 winter and are associated with a low pressure system located over the UK. The strong pressure  
 330 gradient leads to very high wind speeds in the Thames Estuary region. For all of the events, the 1  
 331 minute mean wind speed at both Manston and Shoeburyness exceeds 25 ms<sup>-1</sup> during the period when  
 332 generation is reduced.

333 Three of the five events are characterised by a large reduction in the output as the turbines cut-out  
 334 followed by a similar sized ramp-up. For example, on 25<sup>th</sup> January 2014 at 16:00 there was a  
 335 reduction in capacity factor of the cluster by 28.6% (see Figure 9) which corresponds to a spike in  
 336 wind speeds observed in the region (at Manston, the mean wind speed peaked at 35.5 ms<sup>-1</sup> at 17:30).  
 337 Following this, there is a reduction in wind speeds and therefore the turbines start to generate again  
 338 and therefore there is a ramp-up of 26.7% at 17:00.

339

340

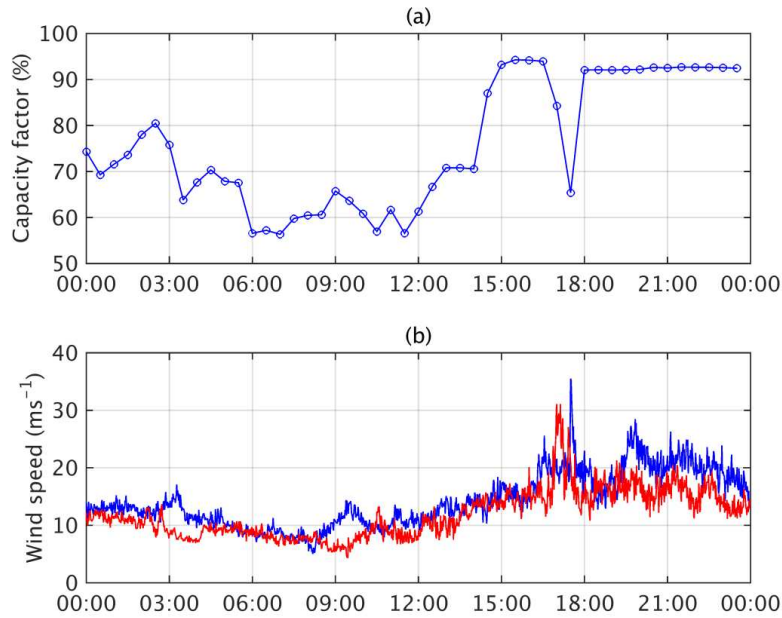
341

342

343  
344  
345  
346  
347  
348

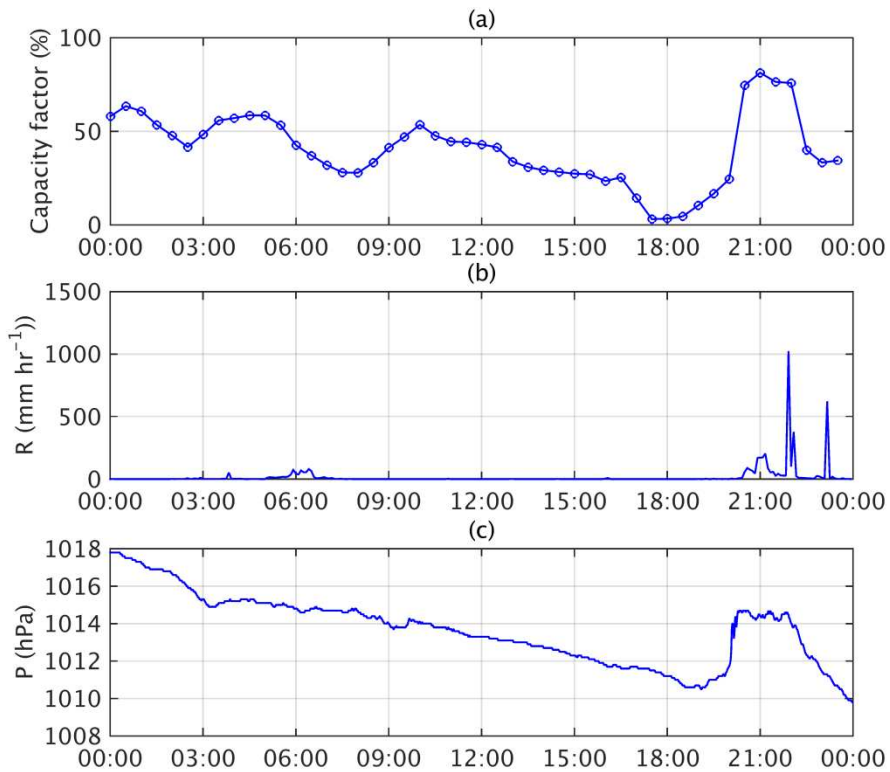
No.	Date	Ramp-up (%) and time	Ramp-down (%) and time	Maximum rainfall rate (mm hr <sup>-1</sup> )	Type
1	25/01	26.7 (17:00)	-28.6 (16:00)	91	Cut-out
2	12/02	38.3 (16:30)	-29.0 (14:00)	15	Cut-out
3	14/02		-44.3 (22:00)	26	Cut-out
4	07/03	27.6 (20:00)		150	Post-frontal
5	23/03	32.6 (16:30)	-28.4 (17:30)	71	Thunderstorms
6	24/05	26.3 (16:30)		97	Post-frontal
7	07/06	45.4 (08:30)	-48.8 (10:00)	12	Thunderstorms
8	18/07	57.9 (19:30)	-42.5 (22:00)	1023	Thunderstorms
9	19/07	39.1 (04:30)	-25.4 (07:00)	64	Thunderstorms
10	19/07	28.6 (19:30)	-28.4 (20:30)	115	Thunderstorms
11	14/08	26.8 (14:30)	-45.9 (15:30)	396	Thunderstorms
12	03/11	31.1 (13:30)	-48.8 (15:30)	147	Post-frontal
13	19/12	36.9 (09:30)	-39.8 (07:00)	622	Cut-out
14	26/12		-36.3 (23:30)	77	Cut-out

**Table 3 Meteorological conditions for the 60 minute ramping events which occurred in the Thames Estuary in 2014 identified using the method outlined in section 2.3.**



349  
350  
351  
352  
353

**Figure 9 Meteorological conditions on 25th January 2014. (a) 30 minute averaged wind power generation of the Thames Estuary cluster (expressed in terms of capacity factor) (b) 1-minute averaged wind speed observations from Manston (blue) and Shoeburyness (red).**



354

355 **Figure 10 Meteorological conditions for the wind power ramping event on 18<sup>th</sup> July 2014. (a) 30 minute averaged**  
 356 **wind power generation of the Thames Estuary cluster (expressed in terms of capacity factor) (b) the maximum**  
 357 **rainfall rate of any gridbox in the Thames Estuary on a 5 minute resolution and (c) 1-minute surface pressure**  
 358 **observations from Manston.**

359

### 360 3.3.4 Thunderstorms

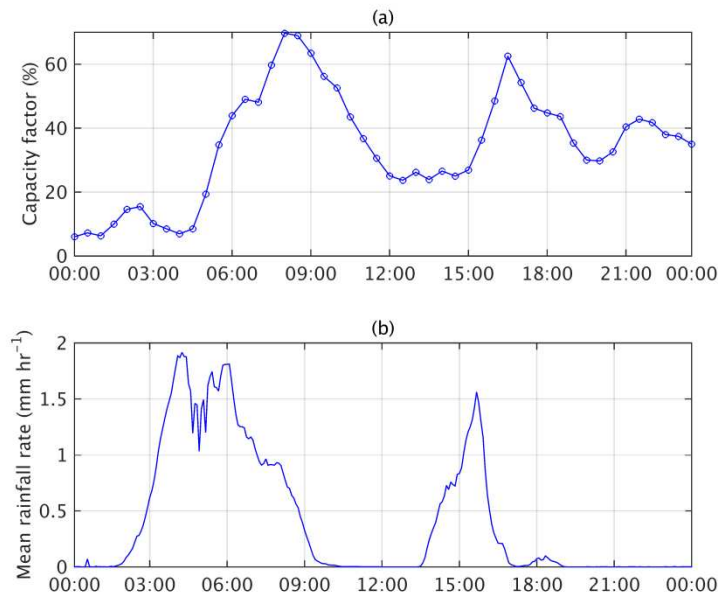
361 There were 6 ramping events **caused by the wind speed gusts** associated with a thunderstorm (2 on  
 362 19<sup>th</sup> July 2014), all of which occurred between March and August. For these events the atmospheric  
 363 conditions are dominated by a high pressure system (anticyclonic) located over the UK and a low  
 364 pressure system to the south west. **Analysis of the meteorological conditions in the Thames Estuary**  
 365 **shows that all ramps coincide with other meteorological conditions which are a signature of the**  
 366 **thunderstorm, such as a period of heavy rainfall in the region and large fluctuations in temperature.**  
 367 For example, the maximum rainfall rate during the ramp for any 1 km radar gridbox in the Thames  
 368 Estuary exceeds 64 mm hr<sup>-1</sup> for all but one of the ramping events. Furthermore, observations at  
 369 Manston and Shoeburyness show there is generally sharp drop in temperature during the ramping  
 370 event.

371 The largest ramping event associated with a thunderstorm occurred on the 18<sup>th</sup> July 2014. At 19:30 the  
 372 capacity factor of the cluster increased by 57.9% (890 MW in 1 hr). **Figure 10** shows this ramp  
 373 coincided with very heavy rainfall across the region. The maximum rainfall rate derived from the  
 374 radar observations was 1023 mm hr<sup>-1</sup> at 22:00. In addition, the surface pressure observed at Manston  
 375 increased by 4 hPa in a 25 minute period (**Figure 10(c)**).

### 376 3.3.5 Post-frontal convection

377 **Three events are caused by a band of increased wind speeds which occur after a front. The elevated**  
 378 **wind speeds lead to an increase in power output from the cluster for a short period of time before the**

379 feature moves away from the region. As with the thunderstorms, there is also a signature of these  
 380 features in the rainfall data. Figure 11 shows the capacity factor of the Thames Estuary wind farms on  
 381 24<sup>th</sup> May 2014 and the mean rainfall rate across the region. During the morning a weather front  
 382 moved across the South East of England which led to high wind speeds and heavy rainfall. After the  
 383 front moved eastwards away from the cluster of farms, their wind generation reduced dramatically,  
 384 falling from 69.7% of capacity at 08:00 to only 23.7% at 13:00. In the mid-afternoon there was an  
 385 increase in wind power generation and by 17:00 the output was back up to 62.6%, however this ramp  
 386 had a short duration and by 20:00 the output had reduced to only 30.0%. Figure 11(b) shows a  
 387 corresponding ramp in the rainfall in the region.



388

389 **Figure 11 Meteorological conditions for the wind power ramping event and the meteorological conditions on 24<sup>th</sup> May**  
 390 **2014. (a) The 30 minute averaged wind power generation of the Thames Estuary cluster (expressed in terms of**  
 391 **capacity factor) and (b) the mean rainfall rate across the Thames Estuary on a 5 minute resolution.**

### 392 3.4 Extreme ramps over 30 time windows

393 For the full year of the data the power ramps over a 30 minute time window have been calculated  
 394 using the method outlined in Section 2.3. The data have then been filtered to remove the periods  
 395 which correspond to a 4 hour ramp (derived in section 3.3.1). As with the 60 minute ramps, Figure 12  
 396 shows that the most extreme 30 minute ramping events are not associated with a larger scale ramp and  
 397 therefore are not caused by the passage of low pressure system but by a smaller scale meteorological  
 398 feature.

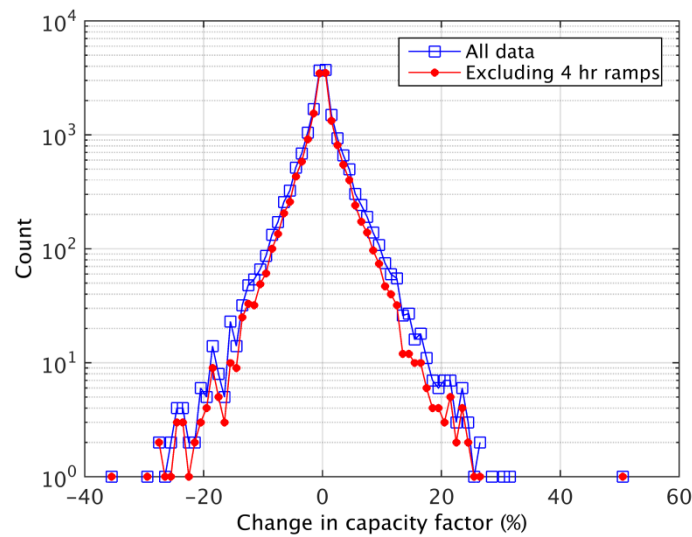
399 Using the method outlined in section 2.3, only 6 30-minute ramping events have been identified (see  
 400 Table 4). For each event, the meteorological mechanism has been determined using a range of  
 401 datasets. Based on the analysis, 4 of the ramps were shown to be associated with the high wind speed  
 402 cut-out of turbines and two are associated with thunderstorms.

403

404  
405  
406

No.	Date	Ramp-up (%) and time	Ramp-down (%) and time	Maximum rainfall rate (mm hr <sup>-1</sup> )	Type
1	03/01		-18.3 (15:30)	9	Cut-out
2	26/01		-16.0 (18:00)	8	Cut-out
3	28/01		-17.4 (04:00)	37	Cut-out
4	01/02	15.2 (07:30)		14	Cut-in
5	19/07	21.3 (08:30)		19	Thunderstorm
6	19/07	16.7 (12:00)		20	Thunderstorm

**Table 4** Details of the 30 minute ramping events which occurred in the Thames Estuary in 2014 identified using the method outlined in section 2.3.



407  
408  
409

**Figure 12** The 30 minute ramps for the Thames Estuary cluster during 2014 using the whole dataset (blue) and then excluding the periods during which a 4 hour ramp occurs.

## 410 4.0 Conclusions

411 In recent years there has been a significant change in the distribution of wind capacity in the UK, with  
412 the construction of several clusters of very large offshore wind farms. This paper investigates how this  
413 change has affected the magnitude of the nationally aggregated and regionalised ramps on temporal  
414 scales which are critical for the management of the power system (30 minute, 60 minute and 4 hours).  
415 In addition, the extreme high frequency ramps of the largest cluster of offshore wind farms (Thames  
416 Estuary) have been investigated in detail to determine the meteorological drivers.

417 Despite the clustering of capacity in relatively small areas, the addition of the offshore wind farms  
418 reduces the high frequency variability of nationally aggregated generation. This study has used two  
419 key parameters to quantify the level of clustering; (1) number of wind farms in the region (2) mean  
420 separation between capacity. The level of the variability has been considered in terms of the  
421 magnitude of the power ramps on the three timescales which are of importance for system  
422 management (30 minutes, 60 minutes and 4 hours). For this metric, the magnitude of the variability  
423 was highly correlated to the number of wind farms aggregated. As the number of wind farms in the  
424 distribution increases, the magnitude of the ramps decreases. This reduction is particularly large  
425 between 5 and 25 wind farms before levelling off as the number of farms increases further. In  
426 contrast, the mean separation between capacity had little impact on the magnitude of the power  
427 swings. In fact, keeping the number of wind farms fixed but changing the separation has a negligible  
428 impact on the standard deviation of the distribution of the power swings. These results show that the  
429 ramps on these time scales in the different regions are not correlated; therefore aggregating the  
430 regions leads to a smoothing effect.



431 As the magnitude of the high frequency power swings are highly dependent on the number of wind  
432 farms, the recent trend in Great Britain for clustering capacity in a small number of very large wind  
433 farms results in an increase in the local power swings. For example, if the system operator were to  
434 hold reserve to protect against a 90<sup>th</sup> percentile swing, for the onshore regions in 2014 it would equate  
435 to on average 3.8%, 6.0% and 14.5% of capacity for 30 minutes, 60 minutes and 4 hours respectively.  
436 In comparison, a similar holding for the offshore regions would equate to an average of 4.8%, 7.9%  
437 and 18.9% of capacity. Consequently, for clusters with high levels of capacity this could lead to very  
438 large ramps in power. For example, for the Thames Estuary, an 18.9% ramp equates to a change in  
439 power of 290 MW. This effect would be exacerbated in the future with the development of even  
440 larger clusters (e.g. Dogger Bank which could have a capacity in excess of 4 GW).

441 The meteorological conditions leading to extreme high frequency ramping of an offshore cluster have  
442 been investigated in more detail using the Thames Estuary as a case study. Over a 4 hour time  
443 window, the largest ramp in capacity factor was 86.2% (which equates to a power swing of 1.3 GW).  
444 This, along with the other extreme 4 hour ramping events was caused by the passage of a cyclone and  
445 the associated weather fronts. On shorter time scales, the largest ramping events over 30 minute and  
446 60 minute time windows are not associated with the passage of fronts. They are caused by three main  
447 meteorological mechanisms; (1) very high wind speeds associated with a cyclone causing turbine cut-  
448 out (2) gusts associated with thunderstorms and (3) organised band of convection following a front.

449 To minimise the balancing costs associated with the extreme high frequency ramping events the  
450 meteorological features need to be captured by the wind power forecast. Drew et al. [3] has shown  
451 that high resolution ensemble models are able to capture the elevated wind speed associated with post-  
452 frontal convection. However, the timing and location of the feature may not be exactly correct. This  
453 study has shown that this problem could potentially be addressed by considering the use of real time  
454 meteorological observations, such as data from the rainfall radar to adjust the forecast in real-time if  
455 necessary.

## 456 Acknowledgements

457 This work was funded by National Grid via the Network Innovation Allowance (NIA\_NGET0128).  
458 The authors would particularly like to thank David Lenaghan (National Grid) for helpful advice  
459 throughout this project and the aggregated wind farm generation data used in this paper. Thanks also  
460 to Dr Rob Thompson from the University of Reading for his assistance with the radar rainfall data.

## 461 References

- 462 1. Department for Business, Energy and Industrial Strategy (2017). Energy Trends June 2017.  
463 Available from <https://www.gov.uk/government/statistics/energy-trends-june-2017>
- 464 2. Heptonstall, P., Gross, R. and Steiner, F. (2016). The costs and impacts of intermittency- 2016  
465 update. UK Energy Research Centre's Technology and Policy Assessment function.
- 466 3. Drew, D.R., Barlow, J. F., Coker, P.J., Frame, T., and Cannon, D.J, (2017) The importance of  
467 forecasting regional wind power ramping: A case study for the UK. *Renewable Energy*, 114,  
468 pp 1201-1208.
- 469 4. Potter, C. W., Gritmit, E., & Nijssen, B. (2009). Rapid Ramp Event Forecast Tool. IEEE  
470 Power systems Conference (pp. 1–5). Seattle, Washington.

- 471 5. Bossavy, A., Girard, R., & Kariniotakis, G. (2013). Forecasting ramps of wind power  
472 production with numerical weather prediction ensembles. *Wind Energy*, (February 2012), 51–  
473 63. doi:10.1002/we
- 474 6. Cutler, N., Kay, M., Jacka, K., & Nielsen, T. S. (2007). Detecting, Categorizing and  
475 Forecasting Large Ramps in Wind Farm Power Output Using Meteorological Observations  
476 and WPPT. *Wind Energy*, (July), 453–470. doi:10.1002/we
- 477 7. Cannon, D. J., Brayshaw, D. J., Methven, J., Coker, P. J., & Lenaghan, D. (2015). Using  
478 reanalysis data to quantify extreme wind power generation statistics: A 33 year case study in  
479 Great Britain. *Renewable Energy*, 75, 767–778. doi:10.1016/j.renene.2014.10.024
- 480 8. Department of Energy and Climate Change (2013). *UK renewable energy roadmap- update*  
481 *2013*. Retrieved from [https://www.gov.uk/government/publications/uk-renewable-energy-](https://www.gov.uk/government/publications/uk-renewable-energy-roadmap-second-update)  
482 [roadmap-second-update](https://www.gov.uk/government/publications/uk-renewable-energy-roadmap-second-update).
- 483 9. RenewableUK. UK Wind Energy Database (UKWED)  
484 [http://www.renewableuk.com/en/renewable-energy/wind-energy/uk-wind-energy-](http://www.renewableuk.com/en/renewable-energy/wind-energy/uk-wind-energy-database/index.cfm)  
485 [database/index.cfm](http://www.renewableuk.com/en/renewable-energy/wind-energy/uk-wind-energy-database/index.cfm) (accessed June 2017).
- 486 10. Higgins, P., & Foley, A. The evolution of offshore wind power in the United Kingdom.  
487 (2014) *Renewable and Sustainable Energy Reviews* 37, 599–612.  
488 doi:10.1016/j.rser.2014.05.058.
- 489 11. National Grid. UK Future energy scenarios. Retrieved from  
490 [http://www2.nationalgrid.com/mediacentral/uk-press-releases/2013/national-grid-s-uk-future-](http://www2.nationalgrid.com/mediacentral/uk-press-releases/2013/national-grid-s-uk-future-energy-scenarios-2013/)  
491 [energy-scenarios-2013/](http://www2.nationalgrid.com/mediacentral/uk-press-releases/2013/national-grid-s-uk-future-energy-scenarios-2013/) 2013.
- 492 12. Drew, D., Cannon, D., Brayshaw, D., Barlow, J., & Coker, P. (2015). The Impact of Future  
493 Offshore Wind Farms on Wind Power Generation in Great Britain. *Resources*, 4(1), 155–171.  
494 doi:10.3390/resources4010155
- 495 13. Vincent, C. L., Pinson, P., & Giebel, G. (2010). Wind fluctuations over the North Sea.  
496 *International Journal of Climatology*, 1595(June 2010), n/a–n/a. doi:10.1002/joc.2175]
- 497 14. Trombe, P., Pinson, P., Vincent, C., Bøvith, T., Cutululis, N. A., Draxl, C., Giebel, G., et al.  
498 (2013). Weather radars – the new eyes for offshore wind farms ? *Wind Energy*, vol 17, no. 11,  
499 pp. 1767–1787, doi:10.1002/we
- 500 15. Kubik, M. L., Brayshaw, D. J., Coker, P. J., & Barlow, J. F. (2013). Exploring the role of  
501 reanalysis data in simulating regional wind generation variability over Northern Ireland.  
502 *Renewable Energy*, 57, 558–561. doi:10.1016/j.renene.2013.02.012
- 503 16. Hurley and Watson (2002). An assessment of the expected variability and load following of a  
504 large wind penetration in Ireland. In proceedings of Global Wind Power Conference. Paris,  
505 France.
- 506 17. Hasche, B. (2010). General statistics of geographically dispersed wind power. *Wind Energy*,  
507 (April), 773–784. doi:10.1002/we330–342.

- 508 18. Giebel, G. (2001). On the benefits of distributed generation of wind energy in Europe.  
509 University of Oldenburg.
- 510 19. Landberg, L. (2007). The availability and variability of the european wind resource.  
511 International Journal of Solar Energy, 18(4), 313–320. doi:10.1080/01425919708914326
- 512 20. Buttler, A., Dinkel, F., Franz, S., & Spliethoff, H. (2016). Variability of wind and solar power  
513 – An assessment of the current situation in the European Union based on the year 2014.  
514 Energy, 106, 147–161. doi:10.1016/j.energy.2016.03.041
- 515 21. Huber, M., Dimkova, D., & Hamacher, T. (2014). Integration of wind and solar power in  
516 Europe: Assessment of flexibility requirements. Energy, 69, 236–246.  
517 doi:10.1016/j.energy.2014.02.109
- 518 22. Sinden, G. (2007). Characteristics of the UK wind resource: Long-term patterns and  
519 relationship to electricity demand. Energy Policy, 35(1), 112–127.  
520 doi:10.1016/j.enpol.2005.10.003
- 521 23. Earl, N., Dorling, S., Hewston, R., & Von Glasow, R. (2013). 1980–2010 Variability in U.K.  
522 Surface Wind Climate. Journal of Climate, 26(4), 1172–1191. doi:10.1175/JCLI-D-12-  
523 00026.1
- 524 24. Cradden, L., Restuccia, F., Hawkins, S., & Harrison, G. (2014). Consideration of wind speed  
525 variability in creating regional aggregate wind power time series. Resources, 3(1), 215–234.  
526 doi:10.3390/resources3010215
- 527 25. Department of Energy and Climate Change. Digest of United Kingdom Energy Statistics  
528 2015; <https://www.gov.uk/government/collections/digest-of-uk-energy-statistics-dukes>, 2015
- 529 26. Met Office (2003): Met Office Rain Radar Data from the NIMROD System. NCAS British  
530 Atmospheric Data Centre,  
531 <http://catalogue.ceda.ac.uk/uuid/82adec1f896af6169112d09cc1174499>
- 532 27. UK Meteorological Office. Met Office integrated data archive system (MIDAS) land surface  
533 station data (1853-current) NCAS British Atmospheric Data Centre. Available from  
534 <http://badc.nerc.ac.uk/>
- 535 28. Rienecker, M. M., Suarez, M. J., Gelaro, R., Todling, R., Bacmeister, J., Liu, E., Bosilovich,  
536 M. G., et al. (2011). MERRA: NASA’s Modern-Era Retrospective Analysis for Research and  
537 Applications. Journal of Climate, 24(14), 3624–3648. doi:10.1175/JCLI-D-11-00015.1.

# 1 Identifying and characterising large ramps in power output of 2 offshore wind farms

3 Daniel. R. Drew<sup>1,\*</sup>, Janet. F. Barlow<sup>1</sup> and Phil. J. Coker<sup>2</sup>

4 <sup>1</sup> Department of Meteorology, University of Reading, Reading, UK

5 <sup>2</sup> School of Construction Management and Engineering, University of Reading, Reading, UK

6 \* Author to whom correspondence should be addressed; E-Mail: d.r.drew@reading.ac.uk;  
7 Tel.: +44 (0)118 378 7696

## 9 Abstract

10 Recently there has been a significant change in the distribution of wind farms in Great Britain with the  
11 construction of clusters of large offshore wind farms. These clusters can produce large ramping events  
12 (i.e. changes in power output) on temporal scales which are critical for managing the power system  
13 (30 minute, 60 minute and 4 hours). This study analyses generation data from the Thames Estuary  
14 cluster in conjunction with meteorological observations to determine the magnitude and frequency of  
15 ramping events and the meteorological mechanism.

16 Over a 4 hour time window, the extreme ramping events of the Thames Estuary cluster were caused  
17 by the passage of a cyclone and associated weather fronts. On shorter time scales, the largest ramping  
18 events over 30 minute and 60 minute time windows are not associated with the passage of fronts.  
19 They are caused by three main meteorological mechanisms; (1) very high wind speeds associated with  
20 a cyclone causing turbine cut-out (2) gusts associated with thunderstorms and (3) organised band of  
21 convection following a front. Despite clustering offshore capacity, the addition of offshore wind farms  
22 has increased the mean separation between capacity and therefore reduced the variability in nationally  
23 aggregated generation on high frequency time scales.

24 Keywords: wind; offshore; variability; ramping; extremes

## 25 1.0 Introduction

26 To meet ambitious carbon reduction targets, global renewable energy deployment has expanded  
27 dramatically. In the UK, the capacity of wind power has grown steadily from 2.9 GW in 2008 to 17.9  
28 GW by June 2017 [1]. Due to the increasing penetration of wind power, extreme wind power  
29 generation events are of growing concern. In particular, ramps in generation provide challenges for  
30 the transmission system operator who schedule reserve holding in advance and require long term  
31 strategies for system balancing [2]. Consequently, a number of studies have focused on understanding  
32 and improving the predictability of wind power ramping events [3, 4, 5, 6].

33 For the UK, Cannon et al. [7] used wind speed data derived from the MERRA reanalysis dataset to  
34 quantify the magnitude and frequency of nationally-aggregated wind generation ramping on time  
35 scales of 6 hours and greater based on the 2012 wind farm distribution. However, in recent years there  
36 has been a significant change in the distribution of wind farms in the Great Britain [8]. Since 2012,  
37 the capacity of offshore wind farms has increased from 2.4 GW to 5.0 GW with much of this capacity  
38 spread over a small number of very large wind farms located in clusters. For example, in the Thames  
39 Estuary alone there is approximately 1.7 GW of capacity. Drew et al. [3] showed this has led to large

40 regional ramps in generation on time scales of minutes to hours as local meteorological phenomena  
41 simultaneously impacts production in several large farms. Given the large capacity of the farms, these  
42 ramps can present a challenge in maintaining the balance between supply and demand on a national  
43 scale, particularly if they are not accurately forecasted.

44 The problem posed by local ramping events is expected to be exacerbated in the coming years, given  
45 the trend for clustering capacity in large offshore wind farms looks set to continue. The latest phase of  
46 offshore wind development in the UK, launched in 2009, identified 9 zones within which a number of  
47 individual wind farms could be located with a total capacity of over 30 GW [9, 10]. Consequently,  
48 following the construction of the round 3 wind farms the majority of GB wind capacity would be  
49 located offshore in clusters of very large wind farms [11, 12].

50 To improve the performance of operational wind power forecasts there is an increasing need for a  
51 clear understanding of the meteorological features responsible for the extreme local ramping events  
52 [13]. For example, Trombe et al. [14] showed that high frequency ramping of large Danish offshore  
53 wind farms can be associated with heavy rainfall and therefore considered the scope for using data  
54 from the rainfall radar to adjust the forecast in real-time if necessary. This study investigates whether  
55 such an approach could be applied to ramping events in the Thames Estuary wind farms.

56 In addition to the problems posed by local ramping events, there are concerns that clustering capacity  
57 could lead to an increase in the variability of the nationally aggregated wind generation (i.e. a reversal  
58 of some of the smoothing benefits gained by the spatial dispersion of turbines). A number of studies  
59 have investigated the reduction in wind power variability due to geographical dispersion of turbines  
60 for single European countries. For example, Kubik et al. for Northern Ireland [15], Hurley and  
61 Watson for Ireland [16], Hasche for Germany and Ireland [17] and Giebel [18], Landberg [19],  
62 Buttler [20] and Huber et al. [21] considered the whole of Europe.

63 For the UK, Sinden [22] and Earl et al. [23] used wind speed data measured at Met Office surface  
64 stations to quantify the inter-annual, seasonal and diurnal variability of UK aggregated wind  
65 generation. However, these studies did not consider offshore sites and assumed the distribution of  
66 wind capacity matched the distribution of weather stations which can lead to large errors [24]. To  
67 address this problem, Cannon et al. [7] used wind speed data derived from the MERRA reanalysis  
68 dataset to determine the characteristics of wind power in Great Britain over a 33 year period. The  
69 study provides a detailed climatology of ramping on time scales of 6 hours and greater.

70 Using the approach outlined in Cannon et al. [7], Drew et al. [12] showed that the increased  
71 penetration of offshore wind farms has little impact on the ramping of GB-aggregated wind  
72 generation on time scales of greater than 6 hours. However, due to the resolution of the model,  
73 MERRA reanalysis data cannot be used to determine the high frequency GB-aggregated power  
74 swings (minutes to hours) or quantify the magnitude of wind power ramps at high spatial resolutions  
75 (below 300 km), both of which are important considerations for managing the power system.

76 In the UK, the electricity market is managed in 30 minute windows, known as settlement periods. For  
77 each period, suppliers and generators contract electricity up to 1 hour prior to the delivery time, a cut-  
78 off time known as “gate closure”. It is then the responsibility of the system operator (National Grid) to  
79 take any necessary actions in order to balance the grid within each settlement period. The electricity  
80 network in the UK is largely isolated with relatively few interconnectors to neighbouring countries  
81 and therefore there is a reliance on large conventional power plants to manage the system. However,  
82 these plants generally require a period of notice prior to generation to ramp up, generally assumed to

83 be at least 4 hours. To manage the power system, it is therefore important to understand the possible  
 84 ramps in power that could occur on time scales shorter than the ramp up time of a conventional power  
 85 plant (4 hours), between gate closure and settlement period (1 hour) and from one settlement period to  
 86 the next (30 minutes).

87 The aim of this study is to use a 30-minute averaged time series of wind power generation from a  
 88 number of regions across Great Britain (GB) in 2014 to investigate how the increased penetration of  
 89 clustered offshore wind capacity has affected the characteristics of generation at high spatial and  
 90 temporal resolutions. The first section considers the impact on high frequency variability of wind  
 91 generation on both a national and regional scale, particularly the magnitude of ramping in generation  
 92 on time scales of less than 4 hours. The second section determines the meteorological causes of  
 93 extreme regional ramping events using the Thames Estuary as a case study.

## 94 2.0 Datasets and analysis methods

95 One of the main challenges when investigating the variability of wind generation in the UK at high  
 96 spatiotemporal resolutions is the limited availability of suitable data. Actual metered data from the  
 97 individual wind farms is protected by commercial interests; therefore there is a reliance on nationally  
 98 aggregated data. However, analysis using this data is unable to quantify the regional power swings or  
 99 indicate how the variability has been affected by the change in wind farm distribution. Cradden et al.  
 100 [24] used an hourly 11 year hindcast derived using the Weather Research and Forecasting model  
 101 (WRF) at 3 km resolution to assess the variability of generation from 13 different regions in the UK.

102 This study introduces a new dataset which details the aggregated power output from four offshore  
 103 clusters (Anglia, Cumbria, N.Wales and Thames) and five onshore regions; Argyll, Ayrshire, Central,  
 104 Lothian and SSENW (see Figure 1) at 30 min resolution from 1<sup>st</sup> January 2014 to 31<sup>st</sup> December 2014  
 105 (see Table 1 and Figure 1). The total capacity across the 9 regions is 6.5 GW, which is approximately  
 106 70% of the total installed wind capacity of Great Britain.

107 A number of wind farms have been excluded from the analysis for two reasons (1) they the sole wind  
 108 farm in a region therefore it was not possible to produce anonymous, aggregated generation data or  
 109 (2) the data was not of sufficient quality. Despite the reduced number of wind farms, the dataset  
 110 provides a good representation of the wind resource. For example, the GB-aggregated capacity factor  
 111 for 2014 was calculated to be 31%, which compares well to the figure of 30.2% for the full wind farm  
 112 distribution [25].

	Mean separation (km)	Number of farms	Capacity (GW)
Lothian	17.3	5	0.44
<b>N.Wales</b>	<b>26.9</b>	<b>3</b>	<b>0.18</b>
<b>Cumbria</b>	<b>30.7</b>	<b>5</b>	<b>1.17</b>
<b>Thames</b>	<b>34.5</b>	<b>4</b>	<b>1.54</b>
<b>Anglia</b>	<b>38.1</b>	<b>3</b>	<b>0.33</b>
Central	60.7	11	1.22
Ayrshire	79.3	8	0.52
Argyll	89.1	6	0.30
SSENW	115.2	16	0.80

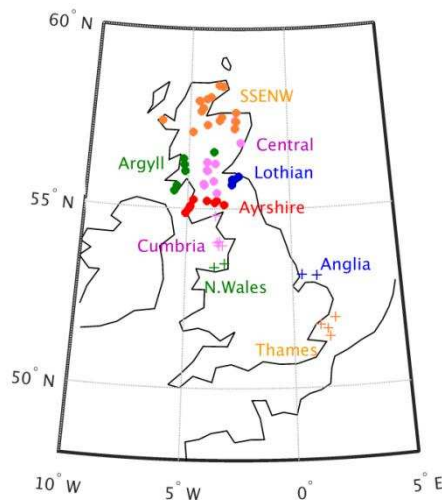
113 **Table 1 Details of the 4 offshore clusters (bold) and the 5 onshore regions. The mean separation is derived using**  
 114 **equation 1 based on the wind farms within each region.**

115 2.1 Spatial separation of capacity

116 The addition of offshore wind farms has changed the distribution of capacity in two distinct ways.  
 117 Firstly, there is an increased concentration of capacity in clusters. For each region the spatial  
 118 dispersion of the capacity has been quantified in terms of the mean separation per unit MW of  
 119 capacity,  $S$ , as calculated in [12] as:

$$s = \sum_{i=1}^N \frac{c_i}{C_T} \left( \sum_{j=1}^N \frac{c_j d_{ij}}{C_T} \right) \quad (1)$$

120 where  $c_j$  is the wind farm capacity,  $d_{ij}$  is the distance between wind farms,  $N$  is the number of wind  
 121 farms in the region and  $C_T$  is the total installed capacity of the region. The offshore regions are  
 122 generally made up of large wind farms clustered together in a relatively small area and consequently  
 123 have a low separation between units of capacity (26.9 km to 38.1 km). In comparison, onshore regions  
 124 generally consist of spatially dispersed small wind farms therefore the separation of the capacity is  
 125 larger (60.7 km to 115.2 km), with the exception of Lothian (17.3 km). Secondly, the addition of the  
 126 offshore regions has changed the geographical location of the generation. Figure 1 shows that all of  
 127 the onshore zones are located relatively close to each other in Scotland; therefore the mean separation  
 128 between the onshore capacity is only 168 km. In contrast, all of the offshore clusters are connected to  
 129 England, and are more geographically dispersed (mean separation of 327.6 km between the offshore  
 130 capacity), therefore by combining the onshore and offshore capacity the mean separation between  
 131 capacity for the GB wind farm distribution increases to 399 km.



132  
 133 **Figure 1 Map of the wind farm distribution used in this study. The onshore and offshore farms are represented by**  
 134 **the circles and crosses respectively.**

135 2.2 Impact of spatial separation on generation characteristics

136 To investigate the impact of spatial separation of capacity on wind power variability in Great Britain,  
 137 the 30-minute averaged time series of aggregated generation for each of the 9 regions have been  
 138 combined to derive a time series of power output for every possible combination of regions. This  
 139 ranges from a combination of two regions (36 possibilities) to the single combination of all nine

140 regions (GB-aggregate) and therefore amounts to a total of 515 possible wind farm distribution  
141 scenarios each with a different number of wind farms and mean separation between capacity. The data  
142 are then used to determine the impact of clustering capacity on the high frequency variability of the  
143 wind generation.

144 A range of different metrics have been used to quantify the variability of wind generation. For the  
145 purposes of this study a ramp,  $R$ , at time,  $t$ , is defined as the difference in the power output over a  
146 period of time,  $\Delta t$ , given by:

$$R(t) = P(t + \Delta t) - P(t) \quad (2)$$

147 where  $P(t)$  is the power output at time,  $t$ . Using the 30-minute averaged dataset, a time series of ramps  
148 for  $\Delta t=30$  minutes, 60 minutes and 4 hours, has been calculated for each wind farm distribution  
149 scenario. The standard deviation,  $\sigma$ , of each time series is then calculated to quantify the distribution  
150 of the ramps for each scenario.

### 151 2.3 Thames Estuary analysis

152 Section 3.3 investigates the most extreme ramping events over three time scales (30 minutes, 60  
153 minutes and 4 hours) of a single offshore cluster in order to determine the meteorological  
154 mechanisms. The analysis focuses on the offshore wind farms in the Thames Estuary, located  
155 approximately 100-200 km east of London, UK. This is the largest of the offshore clusters consisting  
156 of 5 individual farms with a total capacity of 1.7 GW. Drew et al. [3] presents a detailed analysis of a  
157 high frequency ramping event of this cluster which had significant implications on the management of  
158 the power system. This study investigates the full range of extreme ramps to determine the  
159 meteorological cause.

160 To determine extreme ramping events the 30 minute averaged time series of the capacity factor of the  
161 Thames region (as outlined in section 2.2) has been used. The extreme ramping events for each time  
162 window have been defined following a similar method to that outlined in Cutler et al. [6].

- 163 • 4 hour ramps: Find all instances where the 30 minute averaged capacity factor changes by  
164 more than 40% within a 4 hour window. Two individual ramps occurring within a 6 hour  
165 window of each other are considered the same event.
- 166 • 60 minute ramps: After removing the periods of time during which a 4 hour ramp occurs, find  
167 the occasions where the 30 minute averaged capacity factor changes by more than 25% in a  
168 60 minute time window. Two ramps are considered the same event if they occur within 1 hour  
169 of each other.
- 170 • 30 minute ramps: After removing the periods where either a 4 hour or 60 minute ramp occurs,  
171 find the occasions where the 30 minute averaged capacity factor changes by more than 15%  
172 in a 30 minute time window.

173 To determine the meteorological mechanisms behind extreme ramping events, a number of datasets  
174 have been used (Table 2). Firstly, the meteorological conditions in the Thames Estuary region have  
175 been determined using 1-minute averaged observations of temperature, wind speed and surface  
176 pressure from two nearby Met Office weather stations (shown in Figure 2) and rainfall rate data  
177 derived from radar observations for an area of 4884 m<sup>2</sup> covering all of the wind farms on a 1km<sup>2</sup>  
178 spatial resolution and a 5 minute temporal resolution [26, 27]. On the larger scale, the synoptic scale  
179 conditions have been determined using hourly wind fields and surface pressure from Modern-Era  
180 Retrospective Analysis for Research and Applications (MERRA) data [28].

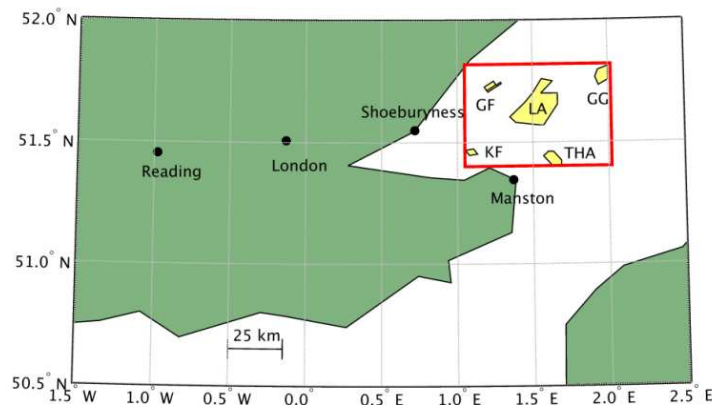


181 In addition to determining the meteorological conditions associated with ramps, hourly surface wind  
 182 field data from MERRA has been used to estimate the aggregated power generation of the wind farms  
 183 in the region, following the method of Cannon et al. [7]. Firstly, the horizontally gridded surface  
 184 hourly winds were bi-linearly interpolated to the location of each wind farm. The derived winds were  
 185 then vertically interpolated to the hub height of the turbines. Finally, the hub-height wind speeds were  
 186 converted to power output using a transfer function derived from empirical comparisons between the  
 187 derived wind speeds and recorded wind farm output. The power output was summed over all wind  
 188 farms to produce an hourly time series of generation of the Thames Estuary cluster.

189

Dataset	Variables	Temporal resolution	Location
UK Met Office weather station observations	Air temperature (C) at 1.25 m above the ground. Mean wind speed and maximum gust at 10 m above the ground ( $\text{ms}^{-1}$ ). Atmospheric pressure (hPa).	1-minute	Manston (51.346°N, 1.337°E).and Shoeburyness (51.536°N, 0.809°E).
Met Office rainfall radar	Rainfall rate ( $\text{mm hr}^{-1}$ )	5-minute	Thames Estuary region (see Figure 2) on $1 \text{ km}^2$ resolution.
MERRA: Modern-Era Retrospective Analysis for Research and Applications	Mean wind speed ( $\text{ms}^{-1}$ ) at heights of 2 m, 10 m and 50 m. Surface pressure (hPa).	Hourly	$0.5^\circ \times 0.667^\circ$ global grid.

190 **Table 1 Details of the meteorological datasets used in this study.**



191

192 **Figure 2 Map showing the location of the 5 wind farms in the Thames Estuary: Greater Gabbard (GG), London**  
 193 **Array (LA), Gunfleet Sands (GF), Kentish Flats (KF) and Thanet (THA). The red box indicates the region for which**  
 194 **radar rainfall data was obtained. The map also shows the locations of the surface meteorological stations: Manston**  
 195 **and Shoeburyness.**

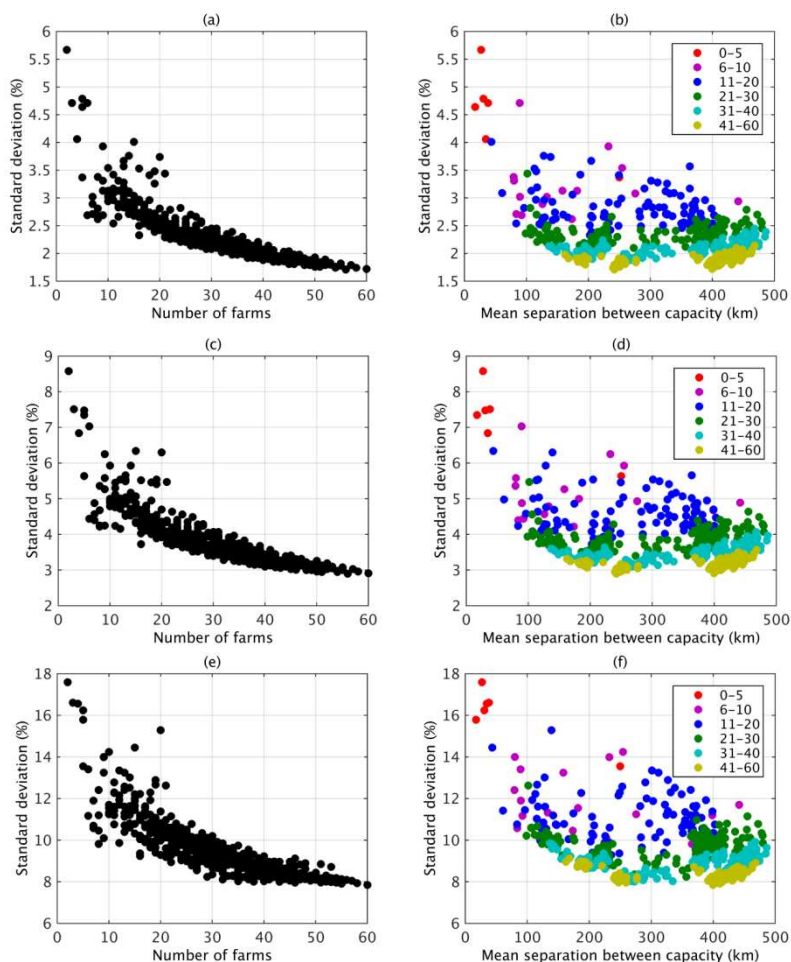
### 196 3.0 Results

197 The dataset outlined in Section 2 has been used to address a series of questions related to wind power  
 198 variability. Section 3.1 investigates the impact of the offshore wind farms on the GB-aggregated wind  
 199 generation characteristics, with a particular emphasis on the impact of changing the separation  
 200 between capacity and the number of wind farms on the magnitude on the high frequency ramps.  
 201 Section 3.2 determines the magnitude of regional high frequency power swings for the offshore

202 clusters and compares the results to that of the more spatially-dispersed onshore regions. Finally,  
 203 Section 3.3 quantifies the high frequency ramping of wind farms in the Thames Estuary, the largest  
 204 offshore cluster and identifies the meteorological mechanism.

### 205 3.1 Impact of clustering capacity on generation variability

206 This section determines how the magnitude of the ramps in regional wind power varies with two  
 207 metrics used to define the level of clustering (1) the number of wind farms aggregated and (2) the  
 208 mean separation between capacity. For all 515 possible wind farm distributions, the time series of  
 209 power ramps over three time periods (30 minutes, 60 minutes and 4 hours) have been determine. The  
 210 standard deviation of the resulting time series was calculated and is used as a measure of the  
 211 magnitude of the ramps.



212  
 213 **Figure 3 Standard deviation of the power ramps of each of the 515 different wind farm distributions as a function of**  
 214 **the number of farms in the distribution and the mean separation between the capacity for three time windows (a)-(b)**  
 215 **30 minutes, (c)-(d) 60 minutes and (e)-(f) 4 hours.**

216 For all three time scales, the magnitude of the ramps decreases as the number of wind farms in the  
 217 distribution increases (see Figures 3(a)-(f)). A large reduction in the standard deviation is shown  
 218 between 5 and 30 wind farms before levelling off as the number of farms increases further. For  
 219 example, for the 30 minute ramps the standard deviation decreases from approximately 4.8% to 2.1%  
 220 as the number of wind farms increases from 5 to 25, but decreases to only 1.9% as the number of  
 221 wind farms increases further to 50. However, for all time scales the lowest standard deviation is  
 222 shown for the largest number of wind farms (i.e. the full GB wind farm distribution).

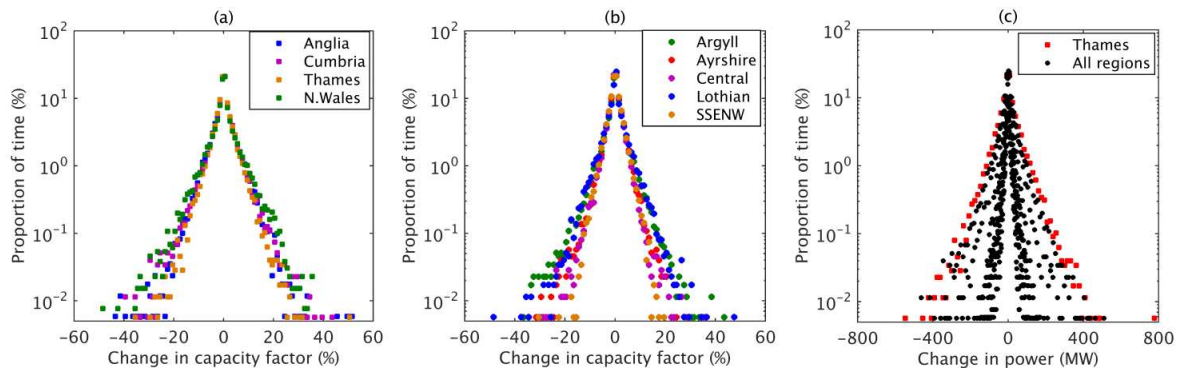
223 This analysis indicates that the number of wind farms aggregated is a useful parameter for estimating  
224 the distribution of power swings on time scales of 30 minutes to 4 hours. In comparison, the  
225 separation between capacity is not a good indicator of the size of the ramps. For all time scales,  
226 increasing the separation (but keeping the number of wind farms the same) has little impact on the  
227 size of the ramps (see Figures 3(b), 3(d) and 3(f). For example, for a wind farm distribution which  
228 contains 41-60 farms, if the separation between the units of capacity is 200 km the standard deviation  
229 of the 30 minute ramps is between 1.8% and 2.0%. If the separation were to increase to 400 km the  
230 standard deviation is very similar (1.7% - 2.0%). These results suggest that on the time scales  
231 considered, the power ramps of the regions are not well correlated, therefore the magnitude of the  
232 aggregated ramps decrease as more and more regions (number of farms) are added, irrespective of any  
233 potential change in the separation between capacity.

### 234 3.2 Regional power ramps

235 The analysis in section 3.2 has shown that the magnitude of the power ramps of a wind farm  
236 distribution is highly dependent on the number of wind farms. The recent trend of concentrating a  
237 small number of very large wind farms therefore results in an increase in the magnitude of the local  
238 power ramps. Figures 4 to 6 show the distribution of the power ramps for each region in Great Britain  
239 in 2014. For all time intervals, the distribution is approximately symmetric with median values close  
240 to zero for both the onshore and offshore regions, indicating that positive and negative ramps have a  
241 similar distribution.

242 In general, when considered in terms of a change in capacity factor, the magnitude of the ramps is  
243 larger for the offshore clusters for all time scales. Consequently, if the system operator were to hold  
244 reserve to protect against a 90th percentile swing, for the onshore regions it would equate to on  
245 average 3.8%, 6.0% and 14.5% of capacity for 30 minutes, 60 minutes and 4 hours respectively. In  
246 comparison a similar holding for the offshore regions would equate to an average of 4.8%, 7.9% and  
247 18.9% of capacity. This is due to the offshore clusters containing a lower number of farms than the  
248 onshore zones. As the 4 offshore regions have a similar number of farms, the magnitude of ramps is  
249 very similar for all offshore regions- with slight differences in the extreme values. For the onshore  
250 regions, there is generally a larger spread in the distributions reflecting the variability in the number of  
251 farms across the regions. For example, for Lothian there are a similar number of wind farms to the  
252 offshore regions and the standard deviation of the ramps is 4.7%, 7.6% and 17.9% for 30 minutes, 60  
253 minutes and 4 hours respectively.

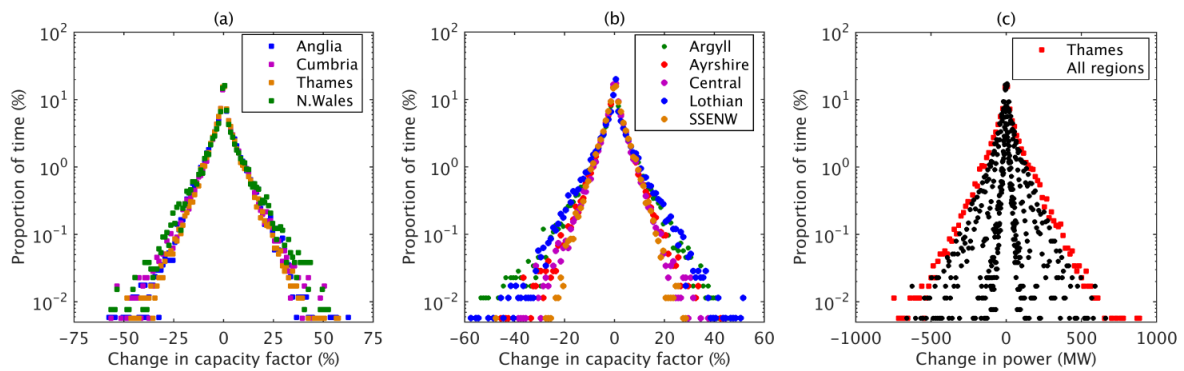
254 When considered in terms of change in power (MW), due to large capacity in Thames Estuary, the  
255 ramps of the cluster are larger than all other regions for all time scales (as shown in Figures 4-6 (c)).  
256 For example, for the 30 minutes, 60 minutes and 4 hour time window, the maximum ramp in the  
257 Thames Estuary is 777 MW, 886 MW and 1363 MW. Power ramps of this magnitude could  
258 potentially pose a challenge to those responsible for maintaining a balance between supply and  
259 demand on the power system. Accurate meteorological forecasting is critical to decisions made on  
260 holding reserve, but can be difficult on such short timescales. Here follows a detailed investigation  
261 into the meteorological conditions causing ramps in the Thames Estuary, to inform development of  
262 accurate forecasts.



263

264  
265

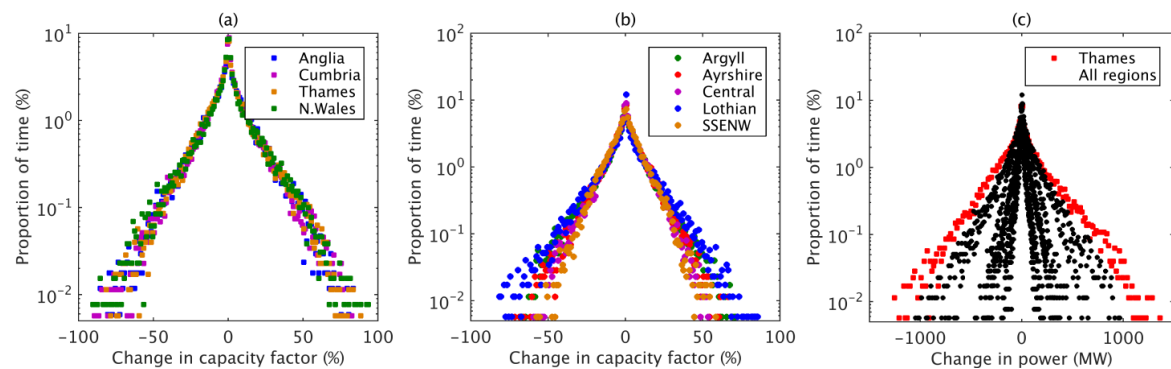
**Figure 4** Distribution of the change in capacity factor within a 30 minute time window in 2014 for (a) offshore clusters (b) onshore regions. (c) The ramps expressed in terms of power (MW).



266

267  
268

**Figure 5** Distribution of the change in capacity factor within a 60 minute time window in 2014 for (a) offshore clusters (b) onshore regions. (c) The ramps expressed in terms of power (MW).



269

270  
271

**Figure 6** Distribution of the change in capacity factor within a 4 hour time window in 2014 for (a) offshore clusters (b) onshore regions. (c) The ramps expressed in terms of power (MW).

### 272 3.3 Thames Estuary ramping

273 In Section 3.2 it was shown that the clusters of offshore wind farms can lead to large high frequency  
 274 regional power ramps. This section analyses the generation data from the Thames Estuary cluster (the  
 275 largest of the offshore clusters in terms of capacity) in more detail, to identify the extreme ramping  
 276 events and determine the meteorological drivers. As with the previous sections, the analysis has been  
 277 completed on three time scales (30 minutes, 60 minutes and 4 hours).

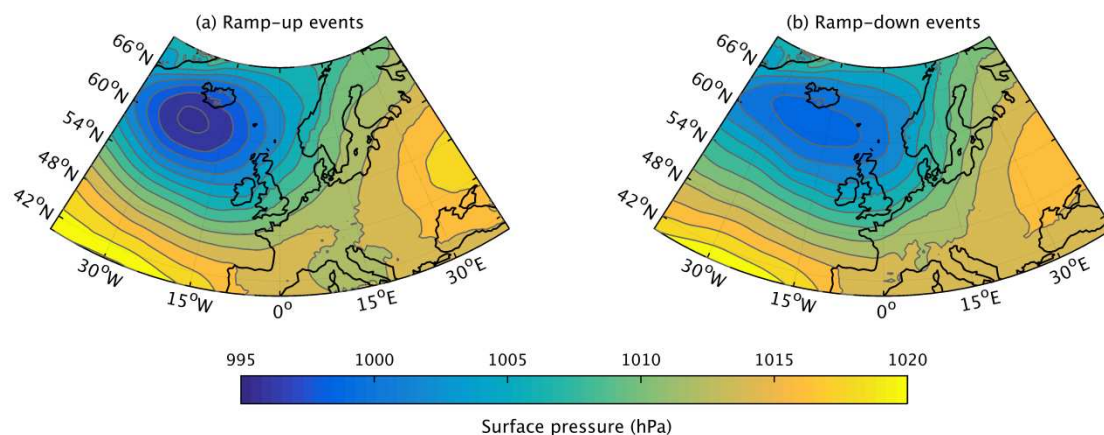
#### 278 3.3.1 Extreme ramps over a 4-hour time window

279 Following the method outlined in section 2.3 (the hourly capacity factor changes by more than 40%  
 280 over a 4 hour time window), 74 ramp-up events and 69 ramp-down events were identified. Events  
 281 occurred throughout the year, however a larger proportion occurred in winter (39% in DJF) than any

282 of the other seasons (22% in MAM, 24% in JJA and 15% in SON). The most extreme ramp-up event  
283 was 86.2% which equates to a change in power of 1.3 GW and the most extreme ramp-down was  
284 76.7% which equates to a change in power of 1.2 GW.

285 For each event, the synoptic meteorological conditions have been investigated using the surface  
286 pressure data from MERRA (see figure 7). All of the extreme ramping events on this time scale can  
287 be linked to the passage of an extra-tropical cyclone (low pressure system) and the associated weather  
288 fronts. For all of the 74 ramp-up events, there is a clear pattern in the surface pressure field. A low  
289 pressure system is centred over Iceland and the frontal features stretch south-east across the UK.  
290 There is a similar pattern for the ramp-down events however the centre of the low pressure has moved  
291 eastwards and the gradient in surface pressure over the UK has weakened. Additionally, the frontal  
292 features are now located east of the cluster.

293 By applying the method developed in Cannon et al. [7], the hourly generation of the Thames Estuary  
294 cluster in 2014 has been estimated based on the surface wind field given by MERRA. The derived  
295 data have been analysed to determine whether extreme ramping events are captured. MERRA is  
296 defined to have captured a ramp if it is at least 75% of the size of the measured ramp within a  $\pm 3$  hour  
297 time window of when it occurred. Based on this criterion, the MERRA derived data captures all 74  
298 ramp-up events and 69 ramp-down events which occurred in the Thames Estuary offshore cluster  
299 during 2014. This confirms that the extreme ramping on this time scale is the result of synoptic scale  
300 meteorological features which are well reproduced by the reanalysis product.

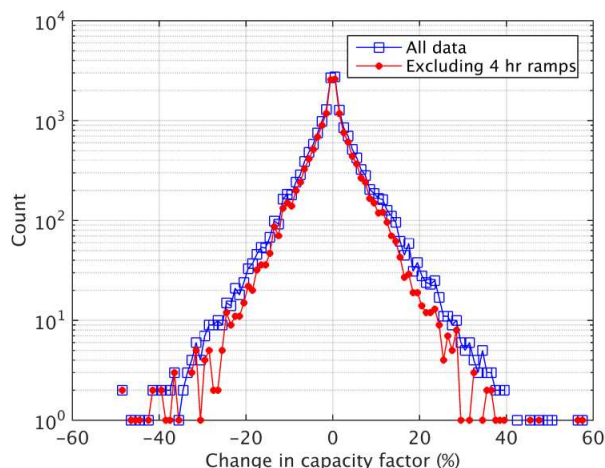


301

302 **Figure 7 Mean sea level pressure averaged across all (a) 74 ramp-up events and (b) 69 ramp-down events.**

### 303 3.3.2 Extreme ramps over a 1-hour time window

304 For the full year of measured data, power ramps over a one hour time window have been calculated  
305 and the frequency distribution of the ramps is shown in Figure 8 (this is the same data as the Thames  
306 curve in Figure 5(a)). The data have then been filtered to remove the periods which contain a 4 hour  
307 ramp (identified in section 3.3.1) and the distribution of the filtered ramps is also shown in Figure 8.  
308 A comparison of the probability density functions shows the most extreme 60 minute ramping events  
309 are the same in both distributions. For the both the filtered and unfiltered datasets the largest ramp-  
310 down is -48.8% and the largest ramp-up event is 57.9%. This indicates that the most extreme 1 hour  
311 ramps are not part of a larger scale ramp and are therefore not caused by the passage of low pressure  
312 system but by smaller scale meteorological features.



313

314 **Figure 8 The 60 minute ramps for the Thames Estuary cluster during 2014 using the whole dataset (blue) and then**  
 315 **excluding the periods during which a 4 hour ramp occurs.**

316 Using the criteria outlined in section 2.3, 24 x 1 hour extreme ramping events have been identified.  
 317 Further analysis shows, on 10 occasions an extreme ramp-up and ramp-down occurred within 3 hours  
 318 of each other (as shown in Table 3). These ramps were combined to produce 14 independent events.  
 319 For each event, the meteorological conditions have been investigated using surface pressure fields  
 320 from MERRA, observations of surface temperature and wind speed from Met Office weather stations  
 321 close to the cluster (Manston and Shoeburyness) and rainfall radar data. Based on the meteorological  
 322 data, 3 main drivers of the extreme ramping on this time scale have been identified; (1) turbine cut-out  
 323 due to high wind speed conditions (2) outflow or gust fronts from thunderstorms and (3) organised  
 324 band of convection following a frontal system.

### 325 3.3.3 High wind speed cut-out

326 There were 5 ramping events associated with the high wind speed shutdown of turbines. The largest  
 327 of which occurred on 14<sup>th</sup> February 2014, when the output of the farms reduced by 44.3% (i.e. a  
 328 reduction in power output of 680 MW in 1 hour). All 5 of the cut-out ramping events occurred in  
 329 winter and are associated with a low pressure system located over the UK. The strong pressure  
 330 gradient leads to very high wind speeds in the Thames Estuary region. For all of the events, the 1  
 331 minute mean wind speed at both Manston and Shoeburyness exceeds 25 ms<sup>-1</sup> during the period when  
 332 generation is reduced.

333 Three of the five events are characterised by a large reduction in the output as the turbines cut-out  
 334 followed by a similar sized ramp-up. For example, on 25<sup>th</sup> January 2014 at 16:00 there was a  
 335 reduction in capacity factor of the cluster by 28.6% (see Figure 9) which corresponds to a spike in  
 336 wind speeds observed in the region (at Manston, the mean wind speed peaked at 35.5 ms<sup>-1</sup> at 17:30).  
 337 Following this, there is a reduction in wind speeds and therefore the turbines start to generate again  
 338 and therefore there is a ramp-up of 26.7% at 17:00.

339

340

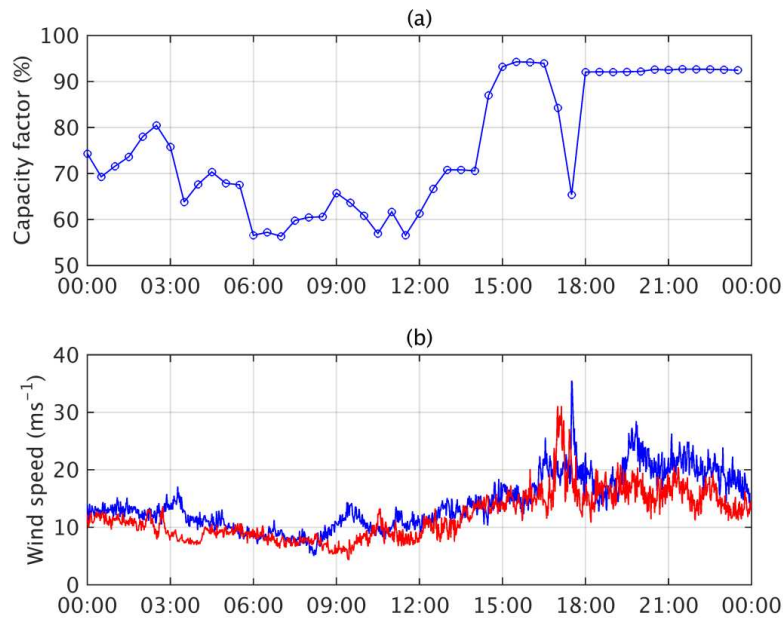
341

342

343  
344  
345  
346  
347  
348

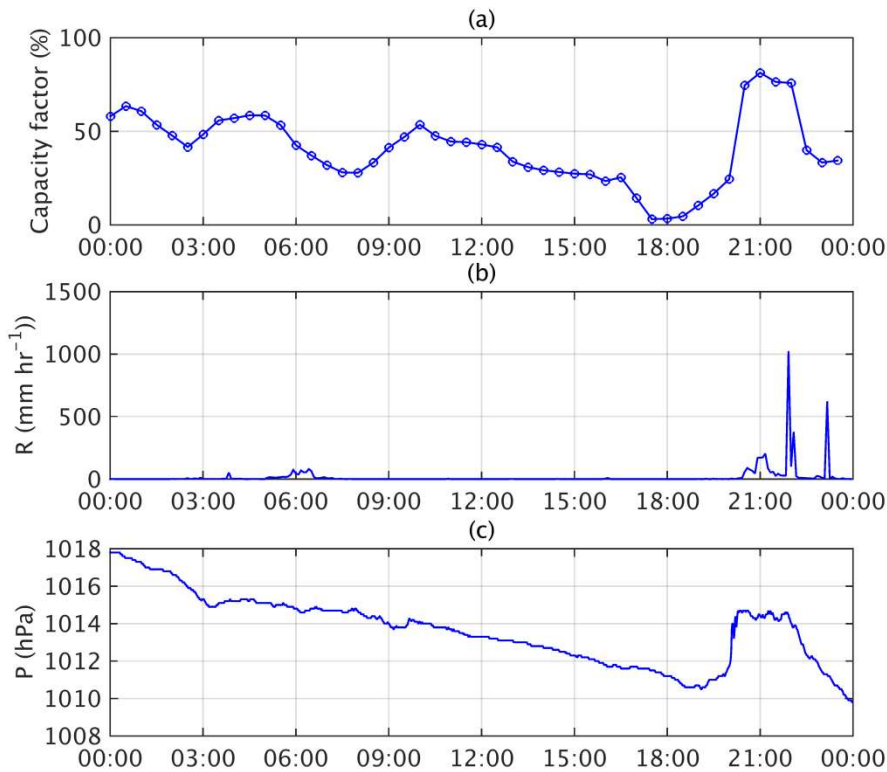
No.	Date	Ramp-up (%) and time	Ramp-down (%) and time	Maximum rainfall rate (mm hr <sup>-1</sup> )	Type
1	25/01	26.7 (17:00)	-28.6 (16:00)	91	Cut-out
2	12/02	38.3 (16:30)	-29.0 (14:00)	15	Cut-out
3	14/02		-44.3 (22:00)	26	Cut-out
4	07/03	27.6 (20:00)		150	Post-frontal
5	23/03	32.6 (16:30)	-28.4 (17:30)	71	Thunderstorms
6	24/05	26.3 (16:30)		97	Post-frontal
7	07/06	45.4 (08:30)	-48.8 (10:00)	12	Thunderstorms
8	18/07	57.9 (19:30)	-42.5 (22:00)	1023	Thunderstorms
9	19/07	39.1 (04:30)	-25.4 (07:00)	64	Thunderstorms
10	19/07	28.6 (19:30)	-28.4 (20:30)	115	Thunderstorms
11	14/08	26.8 (14:30)	-45.9 (15:30)	396	Thunderstorms
12	03/11	31.1 (13:30)	-48.8 (15:30)	147	Post-frontal
13	19/12	36.9 (09:30)	-39.8 (07:00)	622	Cut-out
14	26/12		-36.3 (23:30)	77	Cut-out

Table 3 Meteorological conditions for the 60 minute ramping events which occurred in the Thames Estuary in 2014 identified using the method outlined in section 2.3.



349  
350  
351  
352  
353

Figure 9 Meteorological conditions on 25th January 2014. (a) 30 minute averaged wind power generation of the Thames Estuary cluster (expressed in terms of capacity factor) (b) 1-minute averaged wind speed observations from Manston (blue) and Shoeburyness (red).



354

355 **Figure 10 Meteorological conditions for the wind power ramping event on 18<sup>th</sup> July 2014. (a) 30 minute averaged**  
 356 **wind power generation of the Thames Estuary cluster (expressed in terms of capacity factor) (b) the maximum**  
 357 **rainfall rate of any gridbox in the Thames Estuary on a 5 minute resolution and (c) 1-minute surface pressure**  
 358 **observations from Manston.**

359

### 360 3.3.4 Thunderstorms

361 There were 6 ramping events caused by the wind speed gusts associated with a thunderstorm (2 on  
 362 19<sup>th</sup> July 2014), all of which occurred between March and August. For these events the atmospheric  
 363 conditions are dominated by a high pressure system (anticyclonic) located over the UK and a low  
 364 pressure system to the south west. Analysis of the meteorological conditions in the Thames Estuary  
 365 shows that all ramps coincide with other meteorological conditions which are a signature of the  
 366 thunderstorm, such as a period of heavy rainfall in the region and large fluctuations in temperature.  
 367 For example, the maximum rainfall rate during the ramp for any 1 km radar gridbox in the Thames  
 368 Estuary exceeds 64 mm hr<sup>-1</sup> for all but one of the ramping events. Furthermore, observations at  
 369 Manston and Shoeburyness show there is generally sharp drop in temperature during the ramping  
 370 event.

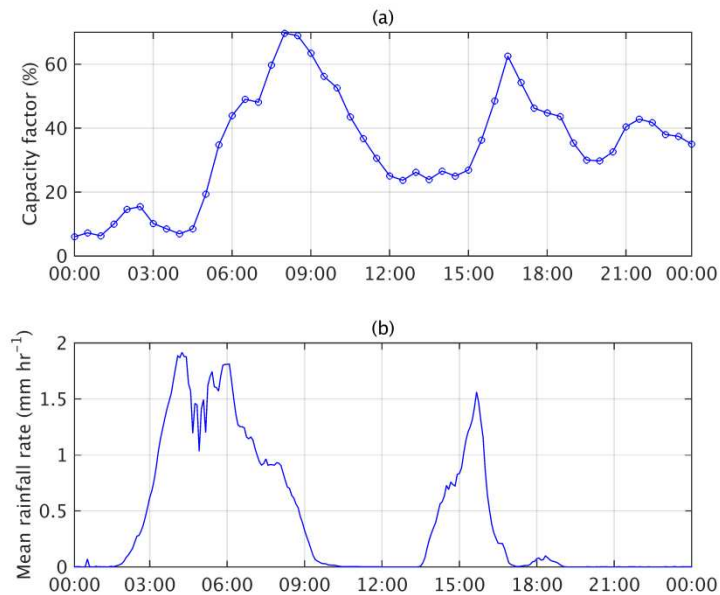
371 The largest ramping event associated with a thunderstorm occurred on the 18<sup>th</sup> July 2014. At 19:30 the  
 372 capacity factor of the cluster increased by 57.9% (890 MW in 1 hr). Figure 10 shows this ramp  
 373 coincided with very heavy rainfall across the region. The maximum rainfall rate derived from the  
 374 radar observations was 1023 mm hr<sup>-1</sup> at 22:00. In addition, the surface pressure observed at Manston  
 375 increased by 4 hPa in a 25 minute period (Figure 10(c)).

### 376 3.3.5 Post-frontal convection

377 Three events are caused by a band of increased wind speeds which occur after a front. The elevated  
 378 wind speeds lead to an increase in power output from the cluster for a short period of time before the



379 feature moves away from the region. As with the thunderstorms, there is also a signature of these  
 380 features in the rainfall data. Figure 11 shows the capacity factor of the Thames Estuary wind farms on  
 381 24<sup>th</sup> May 2014 and the mean rainfall rate across the region. During the morning a weather front  
 382 moved across the South East of England which led to high wind speeds and heavy rainfall. After the  
 383 front moved eastwards away from the cluster of farms, their wind generation reduced dramatically,  
 384 falling from 69.7% of capacity at 08:00 to only 23.7% at 13:00. In the mid-afternoon there was an  
 385 increase in wind power generation and by 17:00 the output was back up to 62.6%, however this ramp  
 386 had a short duration and by 20:00 the output had reduced to only 30.0%. Figure 11(b) shows a  
 387 corresponding ramp in the rainfall in the region.



388

389 **Figure 11 Meteorological conditions for the wind power ramping event and the meteorological conditions on 24<sup>th</sup> May**  
 390 **2014. (a) The 30 minute averaged wind power generation of the Thames Estuary cluster (expressed in terms of**  
 391 **capacity factor) and (b) the mean rainfall rate across the Thames Estuary on a 5 minute resolution.**

### 392 3.4 Extreme ramps over 30 time windows

393 For the full year of the data the power ramps over a 30 minute time window have been calculated  
 394 using the method outlined in Section 2.3. The data have then been filtered to remove the periods  
 395 which correspond to a 4 hour ramp (derived in section 3.3.1). As with the 60 minute ramps, Figure 12  
 396 shows that the most extreme 30 minute ramping events are not associated with a larger scale ramp and  
 397 therefore are not caused by the passage of low pressure system but by a smaller scale meteorological  
 398 feature.

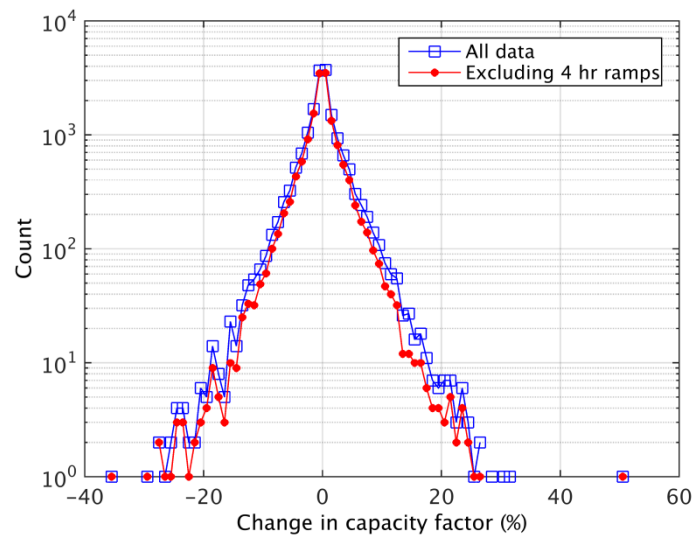
399 Using the method outlined in section 2.3, only 6 30-minute ramping events have been identified (see  
 400 Table 4). For each event, the meteorological mechanism has been determined using a range of  
 401 datasets. Based on the analysis, 4 of the ramps were shown to be associated with the high wind speed  
 402 cut-out of turbines and two are associated with thunderstorms.

403

404  
405  
406

No.	Date	Ramp-up (%) and time	Ramp-down (%) and time	Maximum rainfall rate (mm hr <sup>-1</sup> )	Type
1	03/01		-18.3 (15:30)	9	Cut-out
2	26/01		-16.0 (18:00)	8	Cut-out
3	28/01		-17.4 (04:00)	37	Cut-out
4	01/02	15.2 (07:30)		14	Cut-in
5	19/07	21.3 (08:30)		19	Thunderstorm
6	19/07	16.7 (12:00)		20	Thunderstorm

**Table 4** Details of the 30 minute ramping events which occurred in the Thames Estuary in 2014 identified using the method outlined in section 2.3.



407  
408  
409

**Figure 12** The 30 minute ramps for the Thames Estuary cluster during 2014 using the whole dataset (blue) and then excluding the periods during which a 4 hour ramp occurs.

## 410 4.0 Conclusions

411 In recent years there has been a significant change in the distribution of wind capacity in the UK, with  
412 the construction of several clusters of very large offshore wind farms. This paper investigates how this  
413 change has affected the magnitude of the nationally aggregated and regionalised ramps on temporal  
414 scales which are critical for the management of the power system (30 minute, 60 minute and 4 hours).  
415 In addition, the extreme high frequency ramps of the largest cluster of offshore wind farms (Thames  
416 Estuary) have been investigated in detail to determine the meteorological drivers.

417 Despite the clustering of capacity in relatively small areas, the addition of the offshore wind farms  
418 reduces the high frequency variability of nationally aggregated generation. This study has used two  
419 key parameters to quantify the level of clustering; (1) number of wind farms in the region (2) mean  
420 separation between capacity. The level of the variability has been considered in terms of the  
421 magnitude of the power ramps on the three timescales which are of importance for system  
422 management (30 minutes, 60 minutes and 4 hours). For this metric, the magnitude of the variability  
423 was highly correlated to the number of wind farms aggregated. As the number of wind farms in the  
424 distribution increases, the magnitude of the ramps decreases. This reduction is particularly large  
425 between 5 and 25 wind farms before levelling off as the number of farms increases further. In  
426 contrast, the mean separation between capacity had little impact on the magnitude of the power  
427 swings. In fact, keeping the number of wind farms fixed but changing the separation has a negligible  
428 impact on the standard deviation of the distribution of the power swings. These results show that the  
429 ramps on these time scales in the different regions are not correlated; therefore aggregating the  
430 regions leads to a smoothing effect.

431 As the magnitude of the high frequency power swings are highly dependent on the number of wind  
432 farms, the recent trend in Great Britain for clustering capacity in a small number of very large wind  
433 farms results in an increase in the local power swings. For example, if the system operator were to  
434 hold reserve to protect against a 90<sup>th</sup> percentile swing, for the onshore regions in 2014 it would equate  
435 to on average 3.8%, 6.0% and 14.5% of capacity for 30 minutes, 60 minutes and 4 hours respectively.  
436 In comparison, a similar holding for the offshore regions would equate to an average of 4.8%, 7.9%  
437 and 18.9% of capacity. Consequently, for clusters with high levels of capacity this could lead to very  
438 large ramps in power. For example, for the Thames Estuary, an 18.9% ramp equates to a change in  
439 power of 290 MW. This effect would be exacerbated in the future with the development of even  
440 larger clusters (e.g. Dogger Bank which could have a capacity in excess of 4 GW).

441 The meteorological conditions leading to extreme high frequency ramping of an offshore cluster have  
442 been investigated in more detail using the Thames Estuary as a case study. Over a 4 hour time  
443 window, the largest ramp in capacity factor was 86.2% (which equates to a power swing of 1.3 GW).  
444 This, along with the other extreme 4 hour ramping events was caused by the passage of a cyclone and  
445 the associated weather fronts. On shorter time scales, the largest ramping events over 30 minute and  
446 60 minute time windows are not associated with the passage of fronts. They are caused by three main  
447 meteorological mechanisms; (1) very high wind speeds associated with a cyclone causing turbine cut-  
448 out (2) gusts associated with thunderstorms and (3) organised band of convection following a front.

449 To minimise the balancing costs associated with the extreme high frequency ramping events the  
450 meteorological features need to be captured by the wind power forecast. Drew et al. [3] has shown  
451 that high resolution ensemble models are able to capture the elevated wind speed associated with post-  
452 frontal convection. However, the timing and location of the feature may not be exactly correct. This  
453 study has shown that this problem could potentially be addressed by considering the use of real time  
454 meteorological observations, such as data from the rainfall radar to adjust the forecast in real-time if  
455 necessary.

## 456 Acknowledgements

457 This work was funded by National Grid via the Network Innovation Allowance (NIA\_NGET0128).  
458 The authors would particularly like to thank David Lenaghan (National Grid) for helpful advice  
459 throughout this project and the aggregated wind farm generation data used in this paper. Thanks also  
460 to Dr Rob Thompson from the University of Reading for his assistance with the radar rainfall data.

## 461 References

- 462 1. Department for Business, Energy and Industrial Strategy (2017). Energy Trends June 2017.  
463 Available from <https://www.gov.uk/government/statistics/energy-trends-june-2017>
- 464 2. Heptonstall, P., Gross, R. and Steiner, F. (2016). The costs and impacts of intermittency- 2016  
465 update. UK Energy Research Centre's Technology and Policy Assessment function.
- 466 3. Drew, D.R., Barlow, J. F., Coker, P.J., Frame, T., and Cannon, D.J, (2017) The importance of  
467 forecasting regional wind power ramping: A case study for the UK. *Renewable Energy*, 114,  
468 pp 1201-1208.
- 469 4. Potter, C. W., Gritmit, E., & Nijssen, B. (2009). Rapid Ramp Event Forecast Tool. IEEE  
470 Power systems Conference (pp. 1–5). Seattle, Washington.

- 471 5. Bossavy, A., Girard, R., & Kariniotakis, G. (2013). Forecasting ramps of wind power  
472 production with numerical weather prediction ensembles. *Wind Energy*, (February 2012), 51–  
473 63. doi:10.1002/we
- 474 6. Cutler, N., Kay, M., Jacka, K., & Nielsen, T. S. (2007). Detecting, Categorizing and  
475 Forecasting Large Ramps in Wind Farm Power Output Using Meteorological Observations  
476 and WPPT. *Wind Energy*, (July), 453–470. doi:10.1002/we
- 477 7. Cannon, D. J., Brayshaw, D. J., Methven, J., Coker, P. J., & Lenaghan, D. (2015). Using  
478 reanalysis data to quantify extreme wind power generation statistics: A 33 year case study in  
479 Great Britain. *Renewable Energy*, 75, 767–778. doi:10.1016/j.renene.2014.10.024
- 480 8. Department of Energy and Climate Change (2013). *UK renewable energy roadmap- update*  
481 *2013*. Retrieved from [https://www.gov.uk/government/publications/uk-renewable-energy-](https://www.gov.uk/government/publications/uk-renewable-energy-roadmap-second-update)  
482 [roadmap-second-update](https://www.gov.uk/government/publications/uk-renewable-energy-roadmap-second-update).
- 483 9. RenewableUK. UK Wind Energy Database (UKWED)  
484 [http://www.renewableuk.com/en/renewable-energy/wind-energy/uk-wind-energy-](http://www.renewableuk.com/en/renewable-energy/wind-energy/uk-wind-energy-database/index.cfm)  
485 [database/index.cfm](http://www.renewableuk.com/en/renewable-energy/wind-energy/uk-wind-energy-database/index.cfm) (accessed June 2017).
- 486 10. Higgins, P., & Foley, A. The evolution of offshore wind power in the United Kingdom.  
487 (2014) *Renewable and Sustainable Energy Reviews* 37, 599–612.  
488 doi:10.1016/j.rser.2014.05.058.
- 489 11. National Grid. UK Future energy scenarios. Retrieved from  
490 [http://www2.nationalgrid.com/mediacentral/uk-press-releases/2013/national-grid-s-uk-future-](http://www2.nationalgrid.com/mediacentral/uk-press-releases/2013/national-grid-s-uk-future-energy-scenarios-2013/)  
491 [energy-scenarios-2013/](http://www2.nationalgrid.com/mediacentral/uk-press-releases/2013/national-grid-s-uk-future-energy-scenarios-2013/) 2013.
- 492 12. Drew, D., Cannon, D., Brayshaw, D., Barlow, J., & Coker, P. (2015). The Impact of Future  
493 Offshore Wind Farms on Wind Power Generation in Great Britain. *Resources*, 4(1), 155–171.  
494 doi:10.3390/resources4010155
- 495 13. Vincent, C. L., Pinson, P., & Giebel, G. (2010). Wind fluctuations over the North Sea.  
496 *International Journal of Climatology*, 1595(June 2010), n/a–n/a. doi:10.1002/joc.2175]
- 497 14. Trombe, P., Pinson, P., Vincent, C., Bøvith, T., Cutululis, N. A., Draxl, C., Giebel, G., et al.  
498 (2013). Weather radars – the new eyes for offshore wind farms ? *Wind Energy*, vol 17, no. 11,  
499 pp. 1767–1787, doi:10.1002/we
- 500 15. Kubik, M. L., Brayshaw, D. J., Coker, P. J., & Barlow, J. F. (2013). Exploring the role of  
501 reanalysis data in simulating regional wind generation variability over Northern Ireland.  
502 *Renewable Energy*, 57, 558–561. doi:10.1016/j.renene.2013.02.012
- 503 16. Hurley and Watson (2002). An assessment of the expected variability and load following of a  
504 large wind penetration in Ireland. In proceedings of Global Wind Power Conference. Paris,  
505 France.
- 506 17. Hasche, B. (2010). General statistics of geographically dispersed wind power. *Wind Energy*,  
507 (April), 773–784. doi:10.1002/we330–342.

- 508 18. Giebel, G. (2001). On the benefits of distributed generation of wind energy in Europe.  
509 University of Oldenburg.
- 510 19. Landberg, L. (2007). The availability and variability of the european wind resource.  
511 International Journal of Solar Energy, 18(4), 313–320. doi:10.1080/01425919708914326
- 512 20. Buttler, A., Dinkel, F., Franz, S., & Spliethoff, H. (2016). Variability of wind and solar power  
513 – An assessment of the current situation in the European Union based on the year 2014.  
514 Energy, 106, 147–161. doi:10.1016/j.energy.2016.03.041
- 515 21. Huber, M., Dimkova, D., & Hamacher, T. (2014). Integration of wind and solar power in  
516 Europe: Assessment of flexibility requirements. Energy, 69, 236–246.  
517 doi:10.1016/j.energy.2014.02.109
- 518 22. Sinden, G. (2007). Characteristics of the UK wind resource: Long-term patterns and  
519 relationship to electricity demand. Energy Policy, 35(1), 112–127.  
520 doi:10.1016/j.enpol.2005.10.003
- 521 23. Earl, N., Dorling, S., Hewston, R., & Von Glasow, R. (2013). 1980–2010 Variability in U.K.  
522 Surface Wind Climate. Journal of Climate, 26(4), 1172–1191. doi:10.1175/JCLI-D-12-  
523 00026.1
- 524 24. Cradden, L., Restuccia, F., Hawkins, S., & Harrison, G. (2014). Consideration of wind speed  
525 variability in creating regional aggregate wind power time series. Resources, 3(1), 215–234.  
526 doi:10.3390/resources3010215
- 527 25. Department of Energy and Climate Change. Digest of United Kingdom Energy Statistics  
528 2015; <https://www.gov.uk/government/collections/digest-of-uk-energy-statistics-dukes>, 2015
- 529 26. Met Office (2003): Met Office Rain Radar Data from the NIMROD System. NCAS British  
530 Atmospheric Data Centre,  
531 <http://catalogue.ceda.ac.uk/uuid/82adec1f896af6169112d09cc1174499>
- 532 27. UK Meteorological Office. Met Office integrated data archive system (MIDAS) land surface  
533 station data (1853-current) NCAS British Atmospheric Data Centre. Available from  
534 <http://badc.nerc.ac.uk/>
- 535 28. Rienecker, M. M., Suarez, M. J., Gelaro, R., Todling, R., Bacmeister, J., Liu, E., Bosilovich,  
536 M. G., et al. (2011). MERRA: NASA’s Modern-Era Retrospective Analysis for Research and  
537 Applications. Journal of Climate, 24(14), 3624–3648. doi:10.1175/JCLI-D-11-00015.1.

Figure 1  
[Click here to download high resolution image](#)

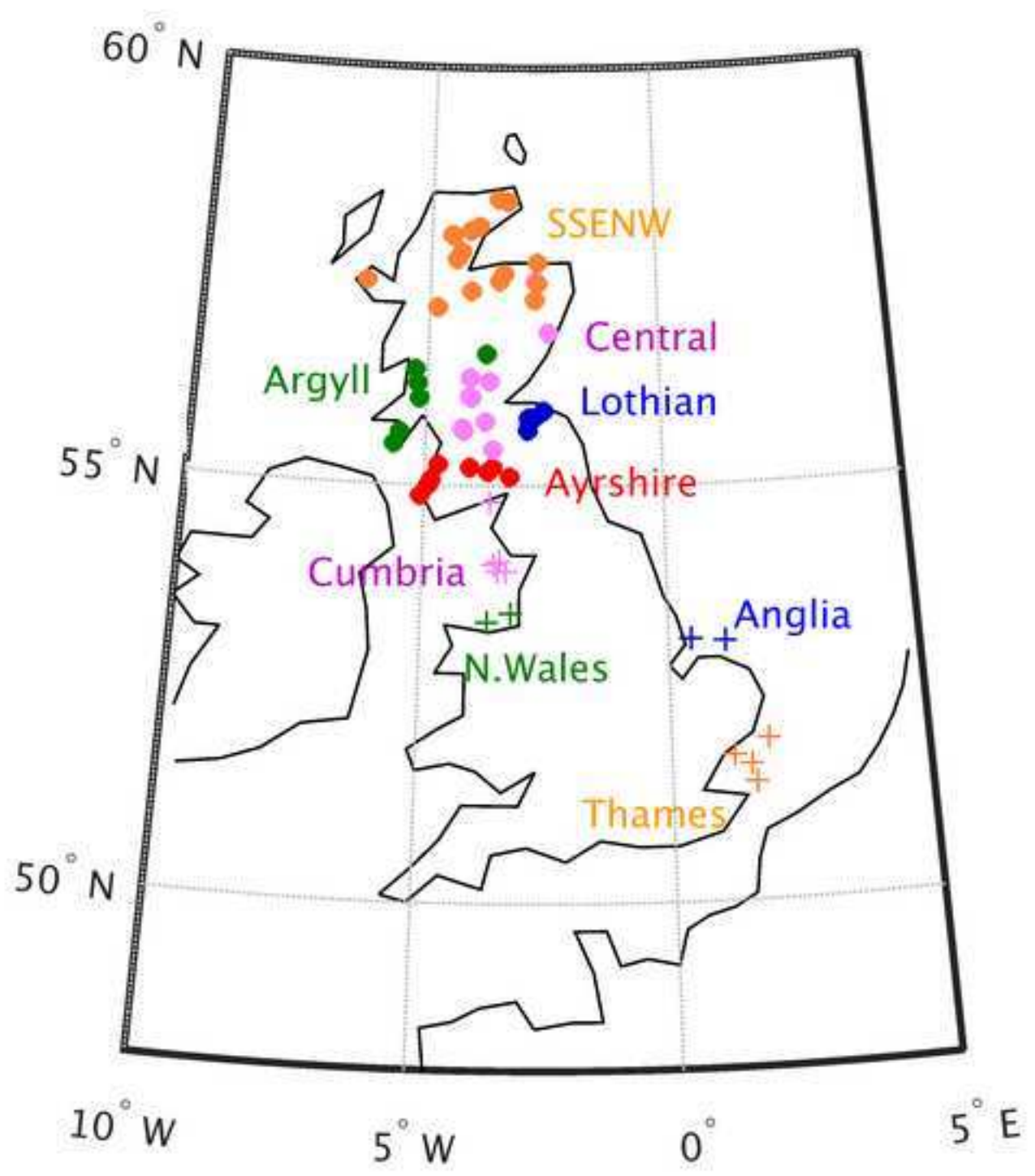


Figure 2  
[Click here to download high resolution image](#)

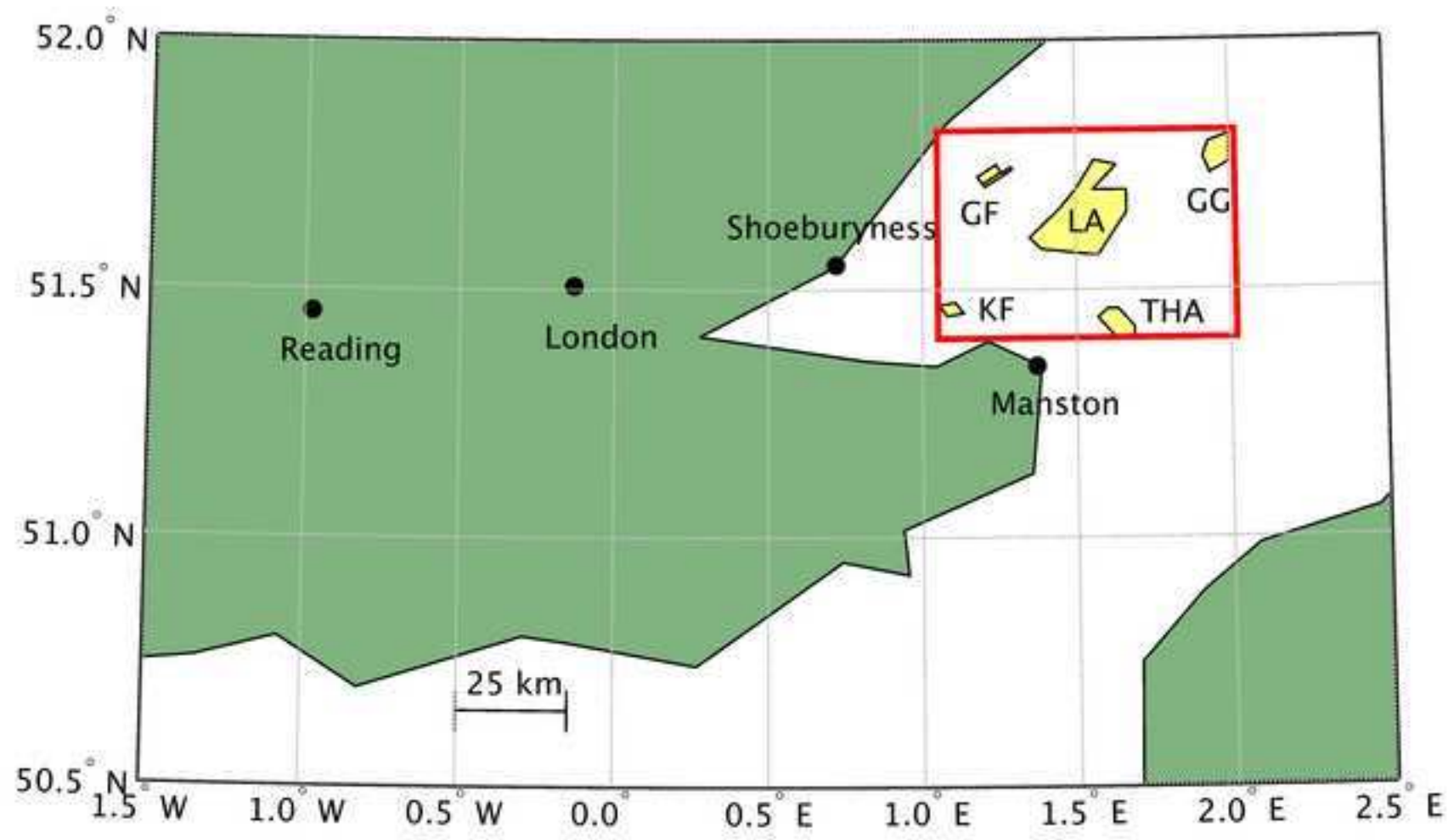


Figure 3  
[Click here to download high resolution image](#)

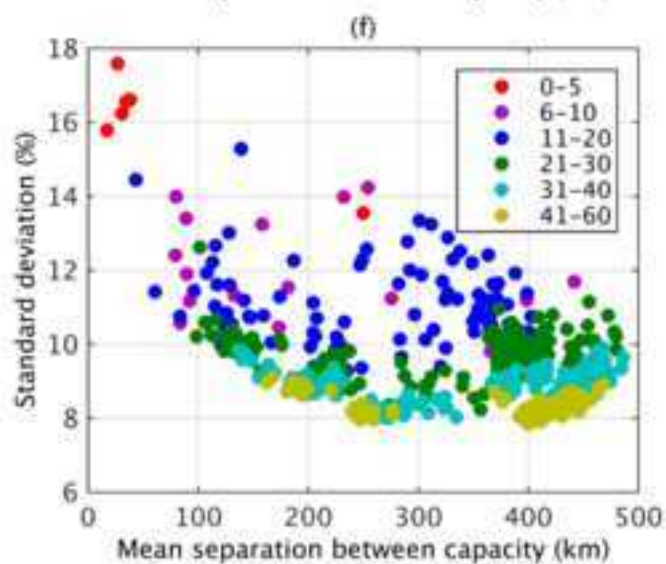
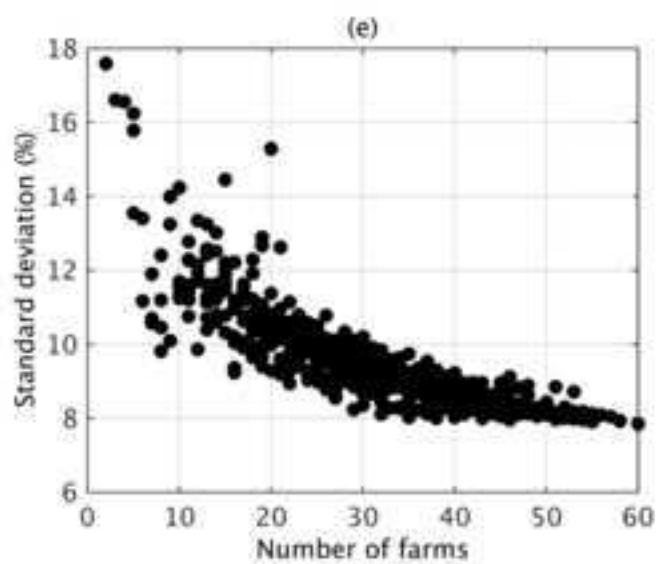
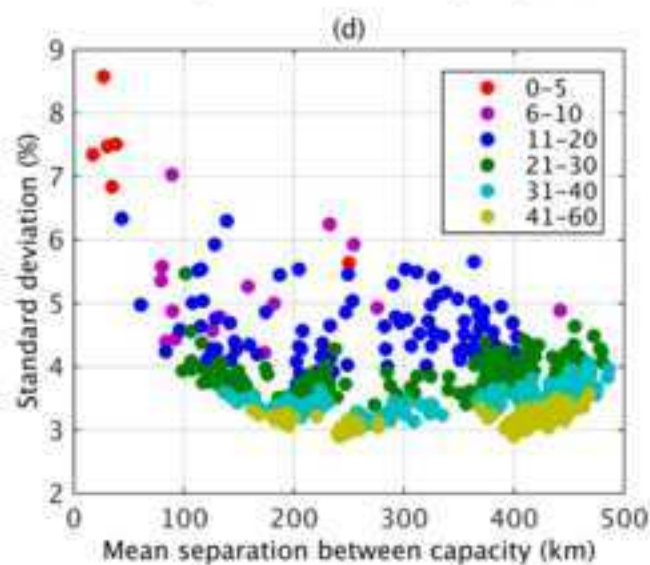
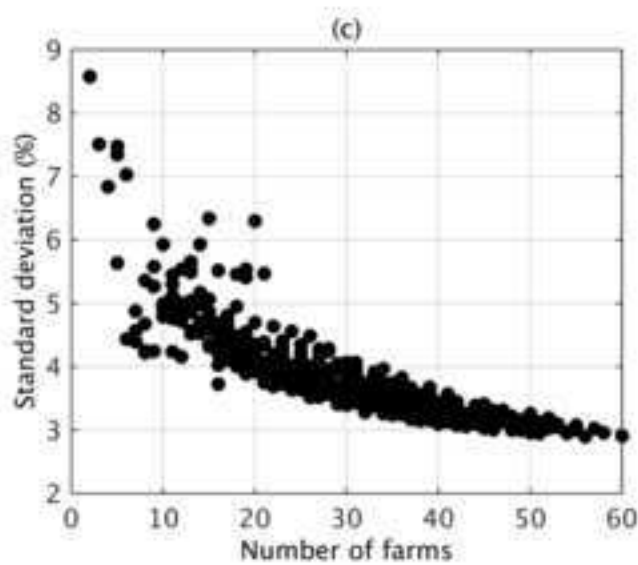
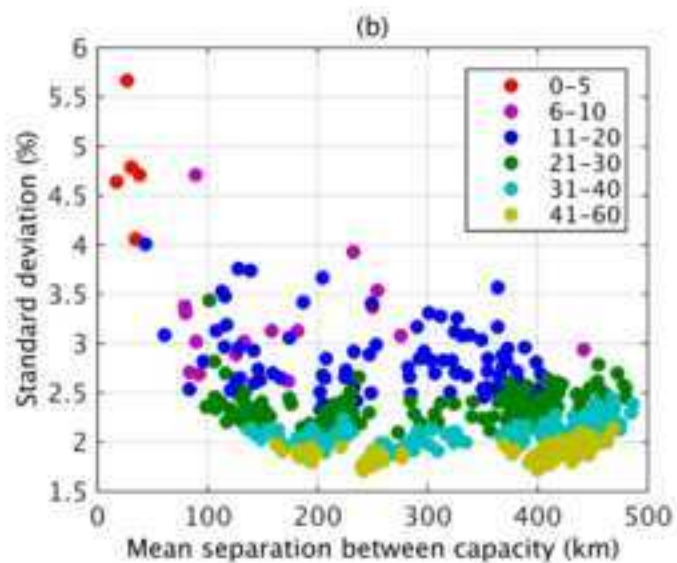
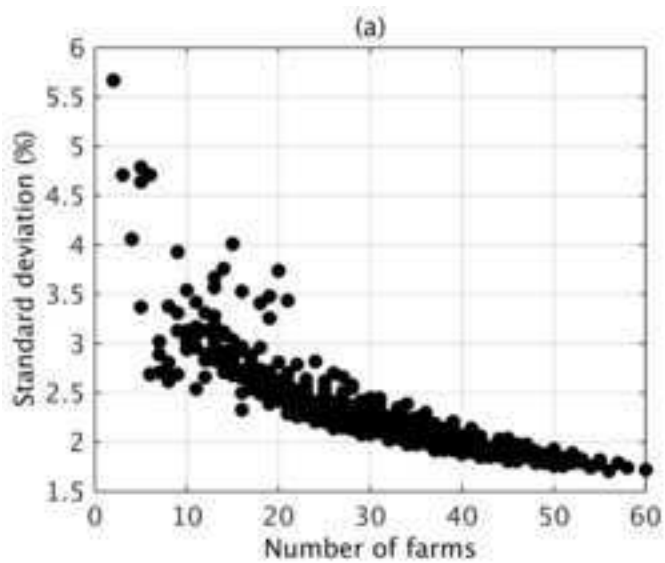




Figure 4  
[Click here to download high resolution image](#)

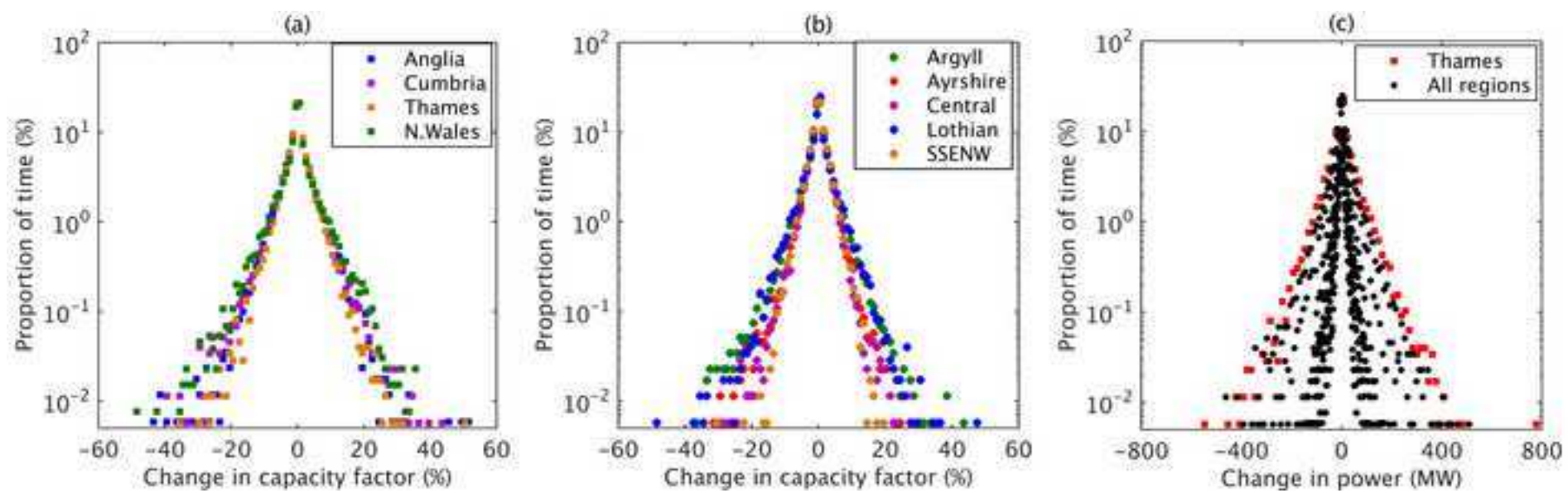


Figure 5  
[Click here to download high resolution image](#)

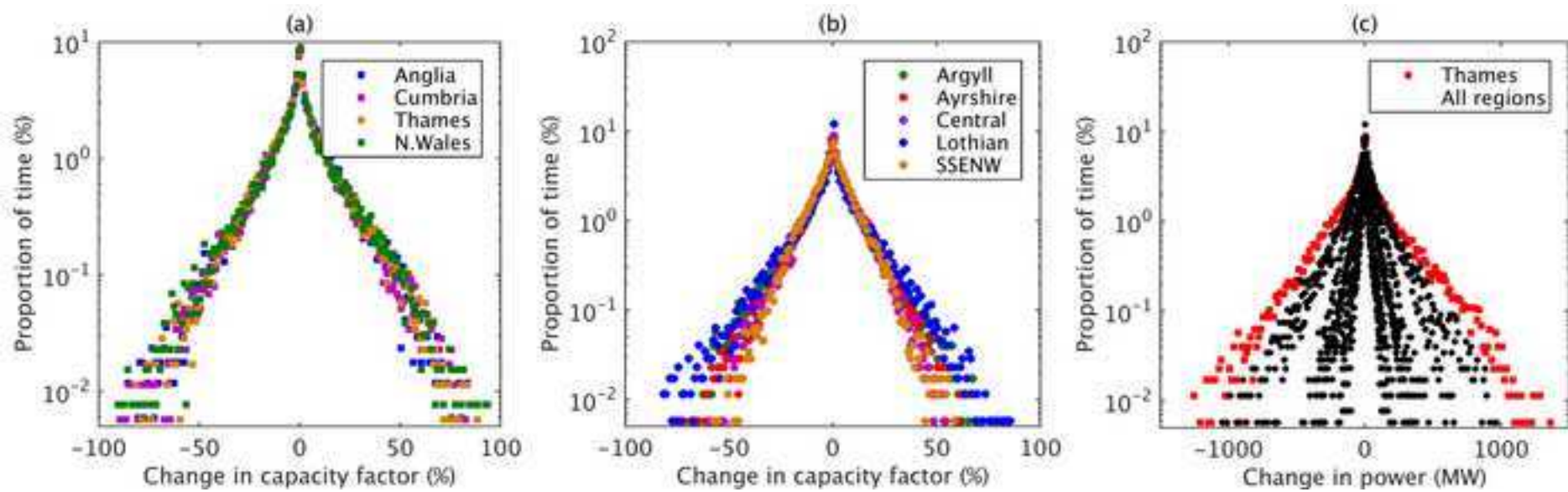


Figure 6  
[Click here to download high resolution image](#)

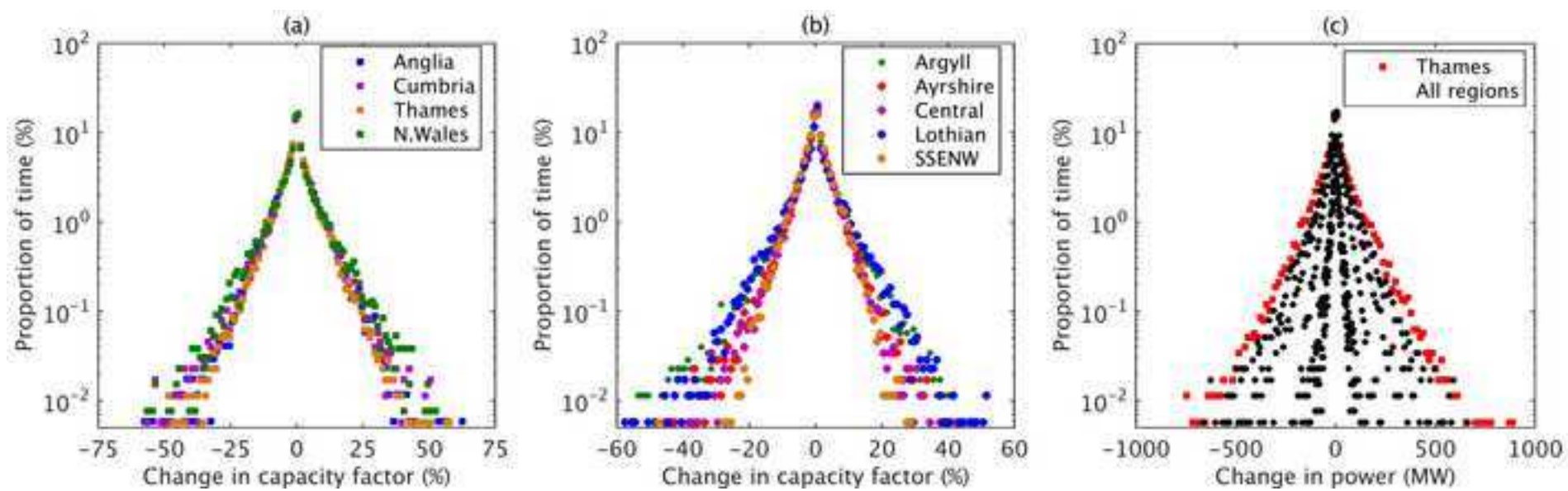


Figure 7  
[Click here to download high resolution image](#)

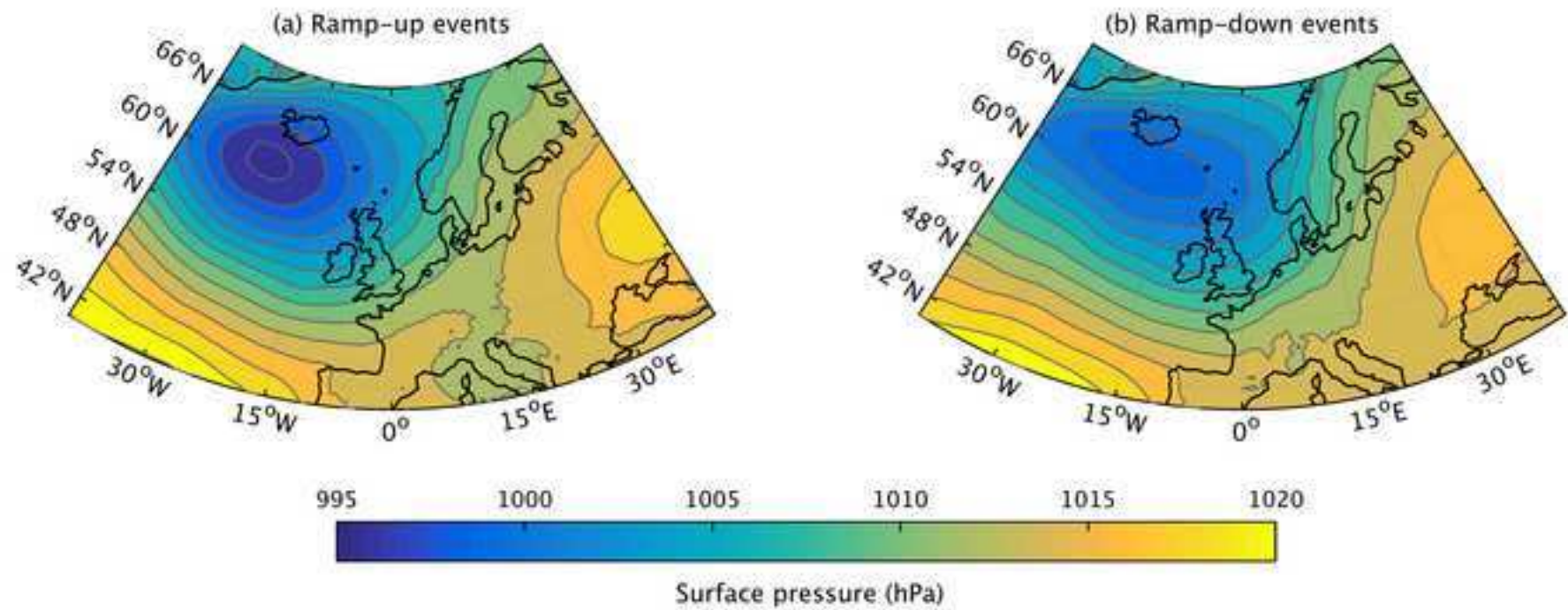


Figure 8  
[Click here to download high resolution image](#)

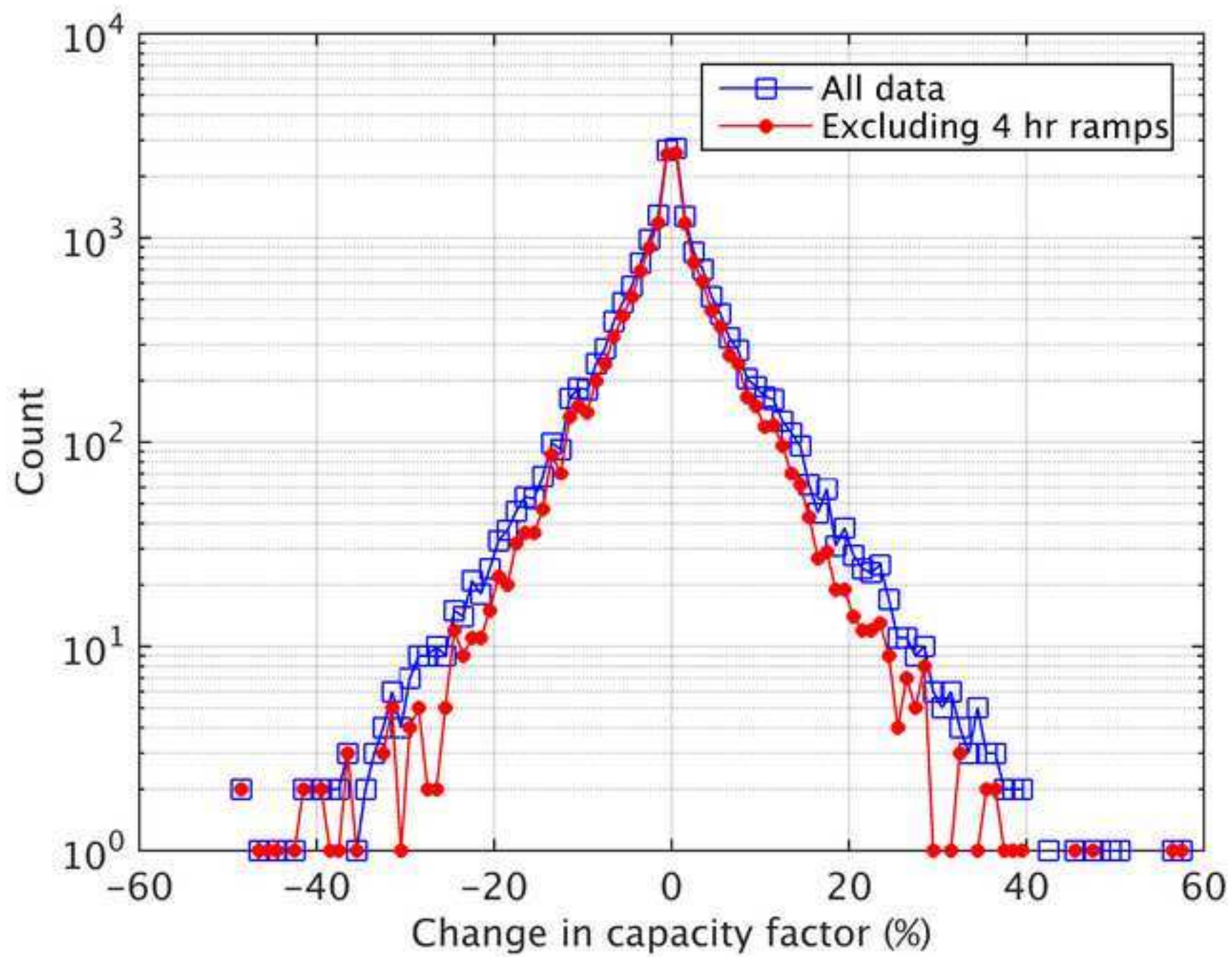


Figure 9  
[Click here to download high resolution image](#)

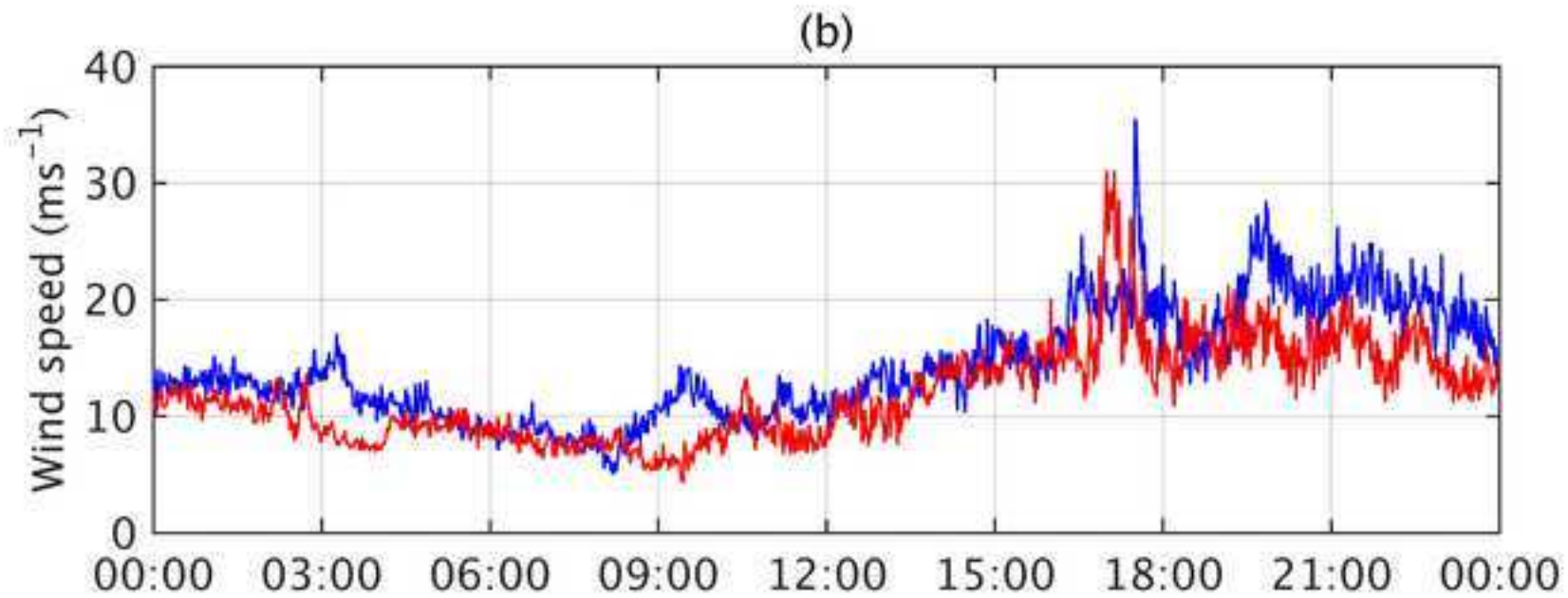
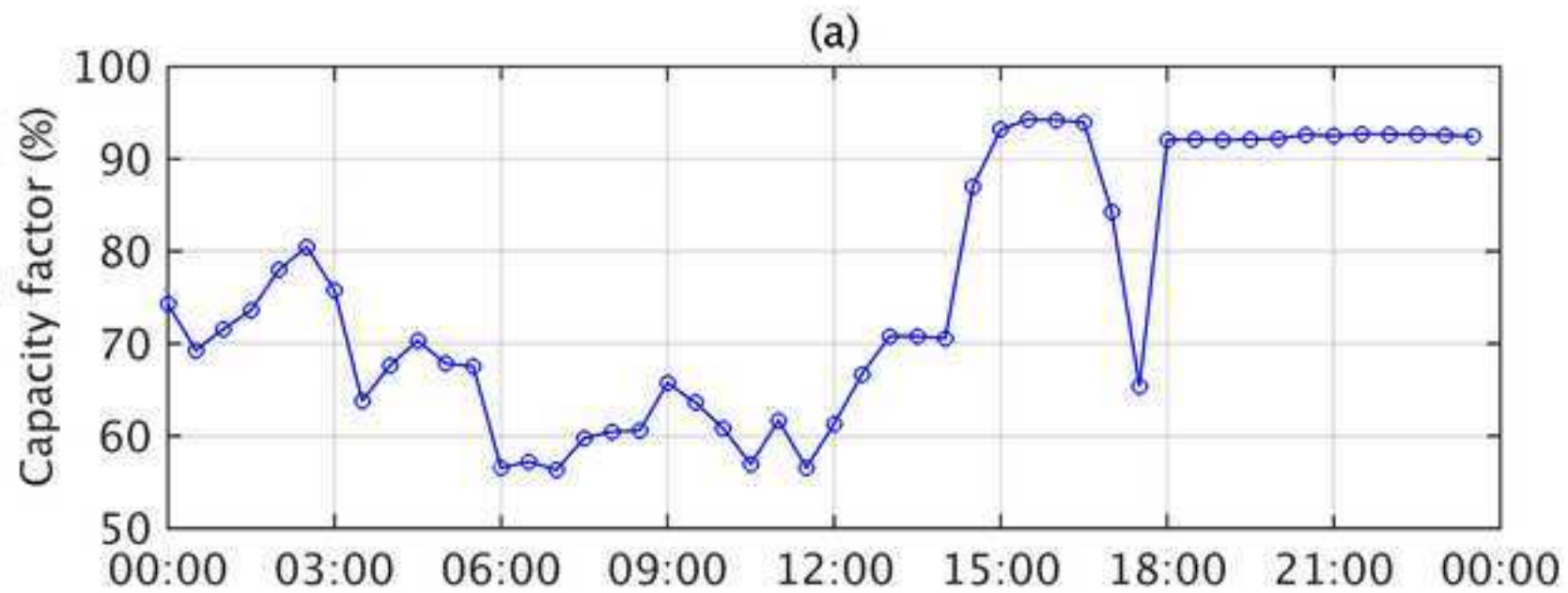


Figure 10  
[Click here to download high resolution image](#)

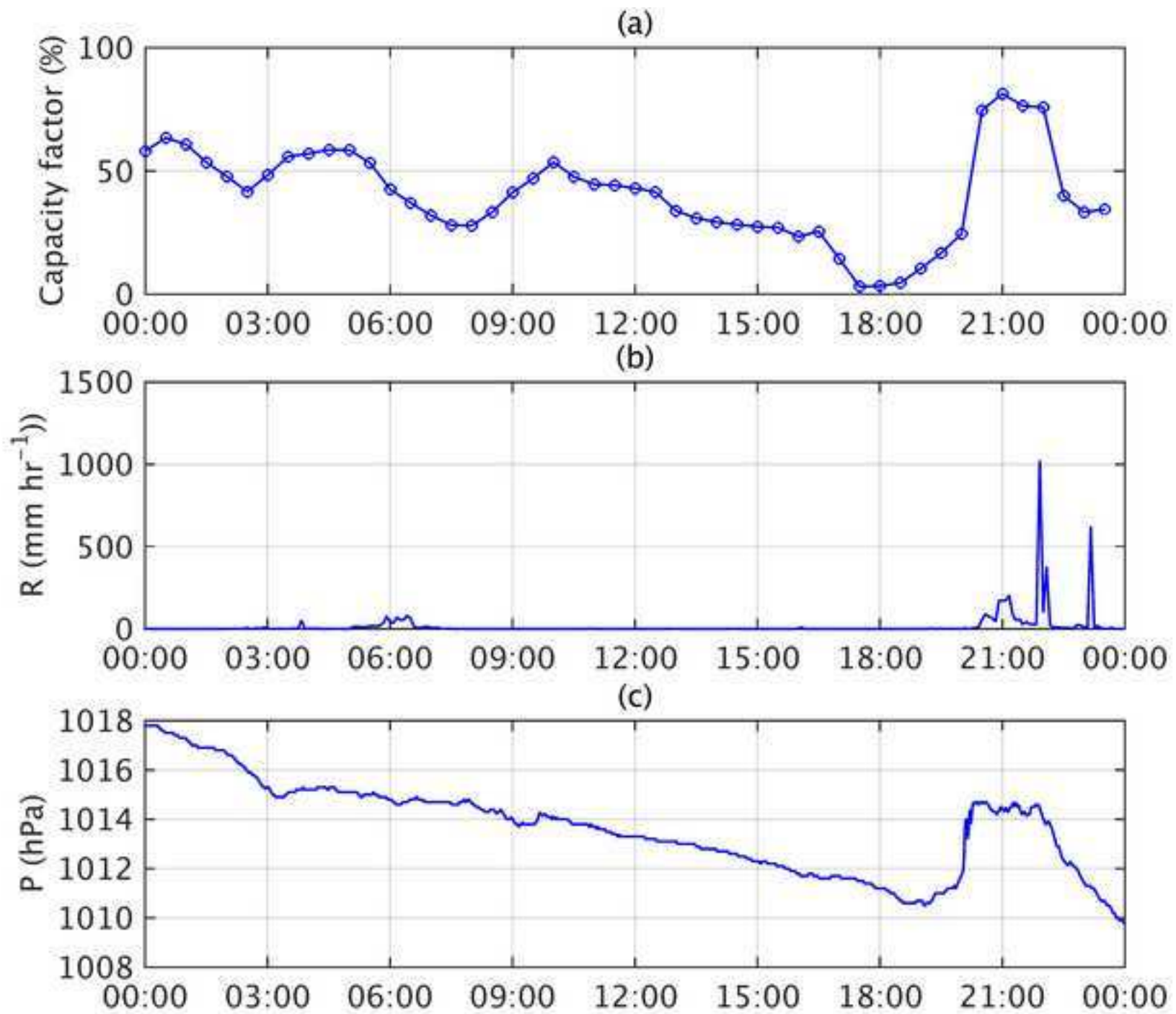


Figure 11  
[Click here to download high resolution image](#)

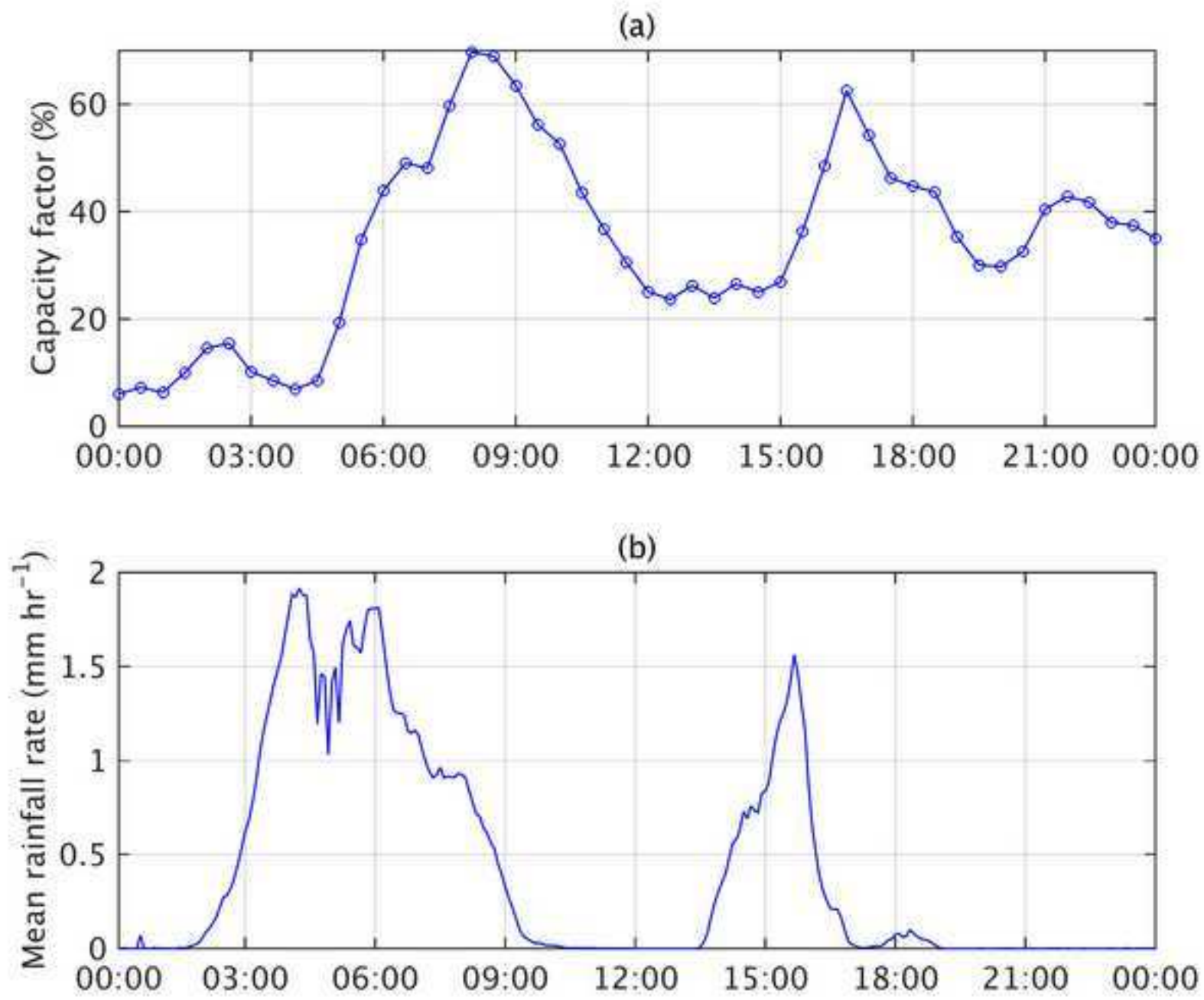




Figure 12  
[Click here to download high resolution image](#)

